2016

Limits on fine texture discrimination in humans and the role of friction

Geetha Pravallika Chimata
Iowa State University

Limits on fine texture discrimination in humans and the role of friction

by

Geetha Pravallika Chimata

A dissertation submitted to the graduate faculty

in partial fulfillment of the requirements for the degree of

DOCTOR OF PHILOSOPHY

Major: Mechanical Engineering

Program of Study Committee:
Christian J Schwartz, Major Professor
Pranav Shrotriya
Sriram Sundararajan
Shana Carpenter
Wei Hong

Iowa State University

Ames, Iowa

2016

DEDICATION

I dedicate this dissertation to my husband Rakesh, for his patience, support and constant encouragement to be the best version of myself; to my parents, Venkata Ratnam and Nageswara Rao, for their boundless love and their multiple sacrifices to make my dreams a reality; and to my ‘second parents’, my aunt Kalavathi and uncle Gangadhara Rao, for their unwavering confidence in me.

TABLE OF CONTENTS

ACKNOWLEDGMENTS

I would like to express my deepest gratitude for my committee chair and advisor Dr. Cris Schwartz for the guidance and wisdom he provided me over this past eight years. I am forever grateful for his patience and support, and for believing in me when I couldn't. This dissertation would not have been possible without his constant help and encouragement.

I would like to thank my committee members Dr. Sriram Sundararajan, Dr. Pranav Shrotriya, Dr. Shana Carpenter and Dr. Wei Hong for their time, kindness and willingness to help with my research.

I am thankful for and would like to acknowledge many others who helped me in this journey: my colleagues Matt Darden, Mark Placette and Thomas Wilde for bouncing ideas with me; Lendie Follett and Jeremy Hadler for the statistics consultations; all my study participants who have been generous with their time; the mechanical engineering department staff who were always willing to go out of their way to help me. This includes, but is not limited to Wyman Martinek, John Howell, Jim Shelledy, Jim Dautremont, Deb Schroeder, Neely Lehman, Nate Jensen and Craig Severson.

Finally, I am thankful to my wonderful in-laws Venkata Ramana, Chandra, Madhuri and Venkat for always being only a phone call away; my friends Jen, Mano and Holly for making my stay in Ames a delight; Akshaya, Praneetha and Raji for being my honest critics, steadfast supporters and constant sources of strength.

CHAPTER 1. GENERAL INTRODUCTION

1.1 Motivation

According to the National Health Interview Survey conducted in 2012, 20.6 million adults in the US reported vision loss [1]. Visual impairment can have significant negative impact on the education and employment options of an induvial. According to the National Foundation for the Blind (NFB) website only 13.7% of people reported with visual disabilities had a bachelor's degree or higher, and of the adults with significant vision loss, only 40.2% were employed[2]. Science, Technology, Engineering and Mathematics (STEM) disciplines have always been challenging for the blind and visually impaired (BVI) and the education statistics in these fields were indicative of this situation. According NSF (national science foundation) report on students with disabilities in STEM fields, only 0.1% total STEM doctorates earned were by visually disabled. Advancements in the assistive technologies (reading machines, refreshable braille displays, braille translation software, braille like display in mobile devices etc.) have been quite helpful. In-spite of these current technologies, there are still major challenges to accessibility of scientific information for the visually challenged. Representation and understanding of diagrams, graphs and, mathematical equations had always been one of the primary obstacles to the BVI students in STEM disciplines. Braille based mathematical notation systems like the Nemeth Braille code offered solution to some these problems, but require considerable effort to train the students and the teachers. Introducing tactile elements (like texture) could increase the information content of the braille without making major changes to its existing communication structure. However, introduction of texture elements requires a thorough investigation of various aspects of tactile perception, including but not limited, to the following:

the discriminability of various textures among themselves, the effect of the texture elements on the perception of braille, the effect of the repeated motion of skin over textured surfaces on the skin (in terms of the skin surface damage).

1.2 Literature Review

1.2.1 Tactile perception

Tactile sensing can be defined as perception through variations in cutaneous stimulations, kinesthetic stimulations or a combination of the both [3]. Human skin is one of the most complex tactile sensing systems known, capable of sensing various forms of sensory inputs such as texture, pressure, vibrations, shape, temperature, and pain. Three different kinds of subcutaneous receptors: mechanoreceptors (pressure or deformation sensitive), thermoreceptors (temperature sensitive) and nociceptors (pain sensitive) in combination with the receptor cells in muscles, joints and tendons called proprioceptors (kinesthetic perception) enable skin to process wide range of tactile sensations. The glabrous skin of the palms, especially on the fingertips, with its very high concentration of mechanoreceptor cells, is particularly adept in processing tactile stimuli, making human hand an ideal tactile sensor[4]. Human hand as sensory system has been studied extensively from neurobiological standpoint through a series of neurophysiological studies and combined psychophysical and neurophysiological studies [5-11]. It was established that there are four types of mechanoreceptor afferents in the hand, each with a specialized perceptual function (sub-modality), and tactile perception results from a combination of these distinctly different functions [12, 13]. However the notion of segregated sub-modalities has been questioned recently and it was suggested that the tactile perception of most of the natural stimuli is a result of the convergent input of multiple sub-modalities[14]. This article indicates that

much remains unclear regarding neurophysiology of touch even with the extensive research in the field. The psychophysics of tactile exploration, which deals with the effect of the physical attributes of the explored object on the sensation of touch, was relatively less studied and even lesser understood.

1.2.2 Texture perception from tactile exploration

Texture of an object, substance, or a liquid is combination of physical attributes such as roughness, hardness, elasticity and viscosity [3]. Perceiving the texture of a surface through touch involves not just the cutaneous inputs, but may include cues from multiple sensory channels including kinesthetic, visual and auditory channels [15]. Yet, texture of a surface can be perceived by vision or auditory channels alone. However, texture perception through touch alone is considered to be superior and preferred channel of perceiving textures, especially for fine textures [16, 17]. A recent study showed that humans can perceive surfaces with nanoscale texture elements [18].

Studies on human evaluation of multiple surfaces encountered in the daily life showed existence of multidimensionality to the tactile perceptual space [19-21]. Further, it was observed that the texture perception was strongly correlated to rough/smooth and soft/hard dimensions and to a lesser extent to the sticky/slippery dimension [19]. Of these three dimensions, the rough/smooth dimension has received the most attention and the “perceived roughness” of the textured surfaces was the focus of most psychophysical studies [22-26].

Most of the psychophysical studies of roughness estimates used gratings and raised dots as stimuli. From the dot pattern and grating studies, the perceived roughness of gratings was known to depend largely on the groove width [23, 26, 27], and the subjective roughness of the

dot patterns varied with the dot diameter and dot spacing [6, 28]. Additionally, there was no evidence of superiority of active touch (finger moves) over passive touch (stimulus moves) in the roughness perception of gratings [27, 29]. Essentially, perceived roughness was greatly affected by surface topography. However, the stimuli in these studies were of coarser textures, with texture elements of dimensions greater than 0.5mm. Hollins et al. showed that the perception of fine textures (element size <100 μm) was greatly enhanced by sliding and surmised the perception of fine textures is fundamentally different from that of the coarse textures [30]. Their findings provided evidence for the "duplex theory of texture perception" proposed by Katz. Katz theorized that spatial mechanisms are involved in the coarse texture perception and vibrotaction is responsible for the fine texture perception [31]. Further, the transition from spacial mechanism mediated perception to the vibrotaction based one was predicted to take place around a spatial period of 200 μm[32]. The perceived roughness of a fine textured surface was proposed to be a function of the Pacinian weighted power of the intensity of the vibrations induced during finger sliding over the surface [32]. The perceived coarseness of printing papers (roughness average Ra < 5 μm) appeared to be related to both the surface roughness and the finger friction coefficient [33].

The hardness of an object can be defined as its ability to resist deformation. Perceived hardness and softness seemed to be inversely related and were in turn related to the measured hardness of the samples [34]. From the neurological standpoint, softness perception seems to involve both cutaneous and kinesthetic cues [35]. The stickiness/slipperiness dimension of texture perception was linked closest to the friction between the finger and a surface. In fact, scaled estimates of stickiness were highly correlated to the measured coefficients of friction [36].

Based on the status of the current literature, it is safe to remark that the hardness and the softness dimensions did not receive as much attention as the roughness.

1.2.3 Texture discrimination through touch

Tactile discrimination of textures involves differentiating surfaces by processing information, possibly about the known dimensions of texture perception such as roughness, hardness and slipperiness of the surface, received through touch. Human sense of touch was proven to be superior to vision for discriminating surfaces, especially of finer textures [16]. Early studies involving discrimination tasks focused on finding height detection thresholds and corresponding neural events for a single raised dot, and noticed that the detection thresholds decreased with an increase in the dot diameter[5, 37]. In a discrimination task involving two dot patterned surfaces, the difference in the spatial period of the surfaces was proportional to the discriminative performance [38]. In a discrimination study involving roughness scaling of gratings, the spacial period was found to be the most relevant dimension for texture discrimination [29]. These studies were quite informative in identifying the dimensions that were important during a discrimination event, but they were limited to only two types of textures (gratings and dot patterns) and rough textures at that. Discrimination tasks were also used to compare the texture perception ability of blind and sighted observers[16, 39]. Miyaoka et al. measured the discrimination thresholds for fine textured surfaces (sandpapers and gratings as stimuli) and proposed that the amplitude information of the roughness profiles was used for tactile discrimination [40]. A more recent study showed that wrinkled surfaces with amplitude as low as 13 nm could be successfully discriminated from blank surfaces, and proposed that the perceptual dimensions involved could be related to the coefficient of friction and the wavelength of the wrinkles [18]. The exact relation between ability to discriminate surfaces and their surface

properties however is undetermined yet. The current literature is lacking in providing a deeper insight into the roles of different perceptual dimensions of the texture and the physical properties of the stimuli in tactile discrimination of texture.

1.2.4 Finger friction and the role of friction in tactile perception

When a finger slides along a stimulus' surface during any tactile exploration activity, there is an inevitable presence of the frictional force from the relative movement. The magnitude and variations in the frictional force are influenced by multiple factors including the topography of the skin and the stimulus, hydration of the skin and the normal load applied and the velocity of sliding [41]. It was observed that the participants during a tactile exploration study, adjusted friction and normal forces for optimal exploration of surface features based on the surface topography [42]. Rate of variation of the friction force was noticed to be strongly correlated to the subjective roughness of a coarse textured surface (truncated conical texture elements of 0.6 mm diameter)[43]. Increased skin friction from perspiration was known to enhance perceived roughness of fabrics [44].

Role of friction in fine texture perception was more marked. Multidimensional analysis of wide range of packaging materials (Roughness average Ra < 15 μm) revealed that the coefficient of friction along with roughness or compliance properties was significantly correlated to wet/dry, sticky/slippery, rough/smooth and bumpy/flat descriptive word pairs (of perception) [21]. Moreover, subjects were capable of accurately scaling friction on a scale of sticky/slippery perception dimension [36]. It was shown that vibrational cues were responsible for fine texture discrimination and furthermore, the perceived roughness of surfaces was a function of the intensity of the vibrations [32]. It was observed for fine textured surfaces with sinusoidal

roughness profiles, that the frequency peak of the vibrations induced by sliding finger over the surface was dependent on the sliding speed and the relative values of the fingerprint dimension and the roughness spatial period [45]. Prevost et al. studied the frequency spectrum of the fluctuations in the friction force as a finger or a fingerlike elastomeric surface scans a randomly textured grating. It was observed by them that the dominant frequency in the spectrum was a function of the scanning speed and the inter-ridge distance of the fingerprints and this frequency falls in the optimal frequency range of the vibration sensitive mechanoreceptors (Pacinian Corpuscles) [46, 47]. Moreover, the amplitude of the oscillating component of the friction force was proportional to the roughness of the stimulus surface [48]. It is quite evident for the existing evidence that friction plays an important role in tactile perception. However, the exact relationship between friction and perception is still not determined. Knowledge of such a relationship can provide for a simple means to control the tactile feel.

1.2.5 Synthetic skin simulants for assessing skin damage

When introducing texture elements into communication language like braille, it is important to consider the possible skin damage during repeated sliding motion of skin over the textured areas. Testing on human subjects to assess the damage can be traumatic to the subjects, expensive, time consuming and can have huge variability in the results. Using a synthetic skin simulant offers an effective solution to counter all the above problems. Synthetic skin when treated with a cosmetic cream exhibited mechanical and tribological properties similar to those of rat skin and showed potential for applications in cosmetic testing [49]. Skin simulants have been successfully used in the past to replicate friction induced skin damage like blistering [50, 51]. However, replicating a skin simulant can be application specific and requires through

understanding of the materials in contact (skin and the textured surface), role of the features of skin on friction, normal load employed and other factors that influence the friction .

The literature overview about tactile perception given here is far from being exhaustive, but demonstrates the need for further study of tactile discrimination of textures from the psychophysical perspective. Better understanding of the role of friction and other physical properties in texture discrimination would enable us to design surfaces whose tactile feel could be precisely controlled according to our needs and takes us closer to achieving the goal of integrating texture elements in Braille.

1.3 Research Objectives and Dissertation Organization

1.3.1 Research objectives

The objective of the current dissertation work is to address the research gap pertaining to the understanding of the discriminative touch of textured surfaces to facilitate the introduction of texture elements into tactile communication languages such as braille. Considering the size of each braille dot (1.44mm), imparting texture to the dots would require use of fine texture elements. Based on these requirements, the research objectives of the current work are classified into two categories:

1. Determining psychophysical factors affecting the discriminatory touch of fine textured surfaces.
    a. To determine the role of surface parameters in fine texture discrimination.
    b. To determine the role of friction in fine texture discrimination.

c. To investigate the effect of the incorporating texture elements on tactile discriminability of braille characters.

2. Developing a testing means for friction induced skin damage due to repetitive motion over textured surfaces.
    a. To determine the factors affecting finger friction during tactile exploration and the specific effects of each of such a factors.
    b. To develop a synthetic skin simulant to assess friction induced skin damage.

1.3.2 Dissertation organization

The chapters in this dissertation are organized according to the chronological order in which the experiments were conducted. Chapters 3 and 5 present the work conducted relevant to the research objective '1' and, Chapters 2 and 4 discuss the work pertaining to the research objective '2'. Specifically, Chapter 2 discusses the development of a layered skin simulant to replicate skin friction blisters, the effect of normal load on the incidence of friction blisters in the simulant and the fracture mechanics modeling of the said skin simulant. Chapter 3 details the research work done to determine the tactile discrimination sensitivity pertaining to non-patterned fine textured surfaces, and to identify a possible correlation to the measured surface and friction properties. Chapter 4 presents results of a study which investigates the effect of the shape, elastic properties and the fingerprints of a finger on fingerpad friction. Chapter 5 details a study conducted to examine the effect of the texture area on tactile discrimination of fine textured surfaces and further explore the role of friction in fine texture discrimination. Chapter 6 summarizes conclusions from all the different studies performed as part of this dissertation research and also discusses the possible directions for future work.

1.4 References

[1] Blackwell, D.L., Lucas, J.W., Clarke, T.C. Summary health statistics for U.S. adults: national health interview survey, 2012. Vital Health Stat 10:1-161 (2014).

[2] Erickson, W., Lee, C., von Schrader, S.: Disability Statistics from the 2013 American Community Survey (ACS). Cornell University Employment and Disability Institute (EDI), Place Cornell University Employment and Disability Institute (EDI) (2015)

[3] Loomis, J.M., Lederman, S.J. Tactual perception. Handbook of perception and human performances 2:2 (1986).

[4] Dargahi, J., Najarian, S.: Human tactile perception as a standard for artificial tactile sensing—a review. pp. 23-35. Place (2004)

[5] LaMotte, R.H., Whitehouse, J. Tactile detection of a dot on a smooth surface: peripheral neural events. Journal of neurophysiology 56:1109 (1986).

[6] Connor, C.E., Hsiao, S.S., Phillips, J.R., Johnson, K.O. Tactile roughness: neural codes that account for psychophysical magnitude estimates. The Journal of Neuroscience 10:3823-3836 (1990).

[7] Srinivasan, M.A., Whitehouse, J.M., LaMotte, R.H. Tactile detection of slip: surface microgeometry and peripheral neural codes. Journal of neurophysiology 63:1323 (1990).

[8] Connor, C.E., Johnson, K.O. Neural coding of tactile texture: comparison of spatial and temporal mechanisms for roughness perception. The Journal of Neuroscience 12:3414-3426 (1992).

[9] Adams, M., Briscoe, B., Johnson, S. Friction and lubrication of human skin. Tribol Lett 26:239-253 (2007).

[10] Johnson, K.O., Phillips, J.R. Tactile spatial resolution. I. Two-point discrimination, gap detection, grating resolution, and letter recognition. Journal of neurophysiology 46:1177-1192 (1981).

[11] Johnson, K.O. Neural mechanisms of tactual forms and texture perception. Annu Rev Neurosci 15:227-250 (1992).

[12] Johnson, K.O., Yoshioka, T., Vega Bermudez, F. Tactile functions of mechanoreceptive afferents innervating the hand. Journal of Clinical Neurophysiology 17:539-558 (2000).

[13] Johnson, K.O. The roles and functions of cutaneous mechanoreceptors. Current Opinion in Neurobiology 11:455-461 (2001).

[14] Saal, H.P., Bensmaia, S.J. Touch is a team effort: interplay of submodalities in cutaneous sensibility. Trends in Neurosciences 37:689-697 (2014).

[15] Lederman , S.J.: The perception of texture by touch. In: W.Schiff, E.Foulke (eds.) Tatual perception: A sourcebook. Cambridge University Press, Place Cambridge University Press (1982)

[16] Heller, M. Texture perception in sighted and blind observers. Perception & Psychophysics 45:49-54 (1989).

[17] Lederman, S.J. Auditory Texture Perception. Perception 8:93-103 (1979).

[18] Skedung, L., Arvidsson, M., Chung, J.Y., Stafford, C.M., Berglund, B., Rutland, M.W. Feeling Small: Exploring the Tactile Perception Limits. Sci Rep 3 (2013).

[19] Hollins, M., Bensmaïa, S., Karlof, K., Young, F. Individual differences in perceptual space for tactile textures: Evidence from multidimensional scaling. Perception & Psychophysics 62:1534-1544 (2000).

[20] Bergmann Tiest, W.M., Kappers, A.M.L. Analysis of haptic perception of materials by multidimensional scaling and physical measurements of roughness and compressibility. Acta Psychologica 121:1-20 (2006).

[21] Chen, X., Shao, F., Barnes, C., Childs, T., Henson, B. Exploring Relationships between Touch Perception and Surface Physical Properties. International Journal of Design 3 (2009).

[22] Lederman, S., Taylor, M. Fingertip force, surface geometry, and the perception of roughness by active touch. Perception & Psychophysics 12:401-408 (1972).

[23] Lederman, S.J. Tactile roughness of grooved surfaces: The touching process and effects of macro- and microsurface structure. Perception & Psychophysics 16:385-395 (1974).

[24] Lederman, S. " Improving one's touch" … and more. Perception & Psychophysics 24:154-160 (1978).

[25] Lederman, S.J., Loomis, J.M., Williams, D.A. The role of vibration in the tactual perception of roughness. Perception & psychophysics 32:109 (1982).

[26] Taylor, M., Lederman, S. Tactile roughness of grooved surfaces: A model and the effect of friction. Perception & Psychophysics 17:23-36 (1975).

[27] Lederman, S.J. Tactual roughness perception: Spatial and temporal determinants. Canadian Journal of Psychology/Revue Canadienne de Psychologie 37:498-511 (1983).

[28] Blake, D.T., Hsiao, S.S., Johnson, K.O. Neural coding mechanisms in tactile pattern recognition: the relative contributions of slowly and rapidly adapting mechanoreceptors to perceived roughness. The Journal of neuroscience : the official journal of the Society for Neuroscience 17:7480 (1997).

[29] Morley, J., Goodwin, A., Darian-Smith, I. Tactile discrimination of gratings. Exp Brain Res 49:291-299 (1983).

[30] Hollins, M., Risner, S.R. Evidence for the duplex theory of tactile texture perception. Perception & Psychophysics 62:695-705 (2000).

[31] Krueger, L.E. David Katz's Der Aufbau der Tastwelt (The world of touch): A synopsis. Perception & Psychophysics 7:337-341 (1970).

[32] Bensmaia, S.J., Hollins, M. The vibrations of texture. Somatosensory & motor research 20:33 (2003).

[33] Skedung, L., Danerlöv, K., Olofsson, U., Michael Johannesson, C., Aikala, M., Kettle, J., et al. Tactile perception: Finger friction, surface roughness and perceived coarseness. Tribology International 44:505-512 (2011).

[34] Harper, R., Stevens, S.S. Subjective hardness of compliant materials. Quarterly Journal of Experimental Psychology 16:204-215 (1964).

[35] Srinivasan, M.A., Lamotte, R.H. Tactual discrimination of softness. Journal of neurophysiology 73:88 (1995).

[36] Smith, A.M., Scott, S.H. Subjective scaling of smooth surface friction. Journal of neurophysiology 75:1957 (1996).

[37] Johansson, R.S., Lamotte, R.H. Tactile detection thresholds for a single asperity on an otherwise smooth surface. Somatosensory & Motor Research 1:21-31 (1983).

[38] Lamb, G.D. Tactile discrimination of textured surfaces: psychophysical performance measurements in humans. The Journal of Physiology 338:551-565 (1983).

[39] Alary, F., Duquette, M., Goldstein, R., Elaine Chapman, C., Voss, P., La Buissonnière-Ariza, V., et al. Tactile acuity in the blind: a closer look reveals superiority over the sighted in some but not all cutaneous tasks. Neuropsychologia 47:2037-2043 (2009).

[40] Miyaoka, T., Mano, T., Ohka, M. Mechanisms of fine-surface-texture discrimination in human tactile sensation. The journal of the acoustical society of America 105:2485-2492 (1999).

[41] Adams, M.J., Johnson, S.A., Lefèvre, P., Lévesque, V., Hayward, V., André, T., et al. Finger pad friction and its role in grip and touch. Journal of The Royal Society Interface 10:20120467 (2013).

[42] Smith, A., Gosselin, G., Houde, B. Deployment of fingertip forces in tactile exploration. Exp Brain Res 147:209-218 (2002).

[43] Smith, A., Chapman, C., Deslandes, M., Langlais, J.-S., Thibodeau, M.-P. Role of friction and tangential force variation in the subjective scaling of tactile roughness. Exp Brain Res 144:211-223 (2002).

[44] Gwosdow, A.R., Stevens, J.C., Berglund, L.G., Stolwijk, J.A.J. Skin Friction and Fabric Sensations in Neutral and Warm Environments. Textile Research Journal 56:574-580 (1986).

[45] Fagiani, R., Massi, F., Chatelet, E., Berthier, Y., Akay, A. Tactile perception by friction induced vibrations. Tribology International 44:1100-1110 (2011).

[46] Prevost, A., Scheibert, J., Debrégeas, G. Effect of fingerprints orientation on skin vibrations during tactile exploration of textured surfaces. Communicative & integrative biology 2:422 (2009).

[47] Scheibert, J., Leurent, S., Prevost, A., Debrégeas, G. The role of fingerprints in the coding of tactile information probed with a biomimetic sensor. Science (New York, NY) 323:1503 (2009).

[48] Wandersman, E., Candelier, R., Debrégeas, G., Prevost, A. Texture- induced modulations of friction force: the fingerprint effect. Physical review letters 107:164301 (2011).

[49] Bhushan, B., Tang, W. Surface, tribological, and mechanical characterization of synthetic skins for tribological applications in cosmetic science. Journal of applied polymer science 120:2881-2890 (2011).

[50] Chimata, G.P., Schwartz, C.J. Investigation of the effect of the normal load on the incidence of friction blisters in a skin-simulant model. Proceedings of the Institution of Mechanical Engineers, Part J: Journal of Engineering Tribology (2014).

[51] Guerra, C., Schwartz, C. Development of a Synthetic Skin Simulant Platform for the Investigation of Dermal Blistering Mechanics. Tribol Lett 44:223-228 (2011).

CHAPTER 2. INVESTIGATION OF THE EFFECT OF THE NORMAL LOAD ON THE INCIDENCE OF FRICTION BLISTERS IN A SKIN-SIMULANT MODEL

A paper published in Journal of Engineering Tribology.

G.P. Chimata and C.J. Schwartz

Abstract

A laminar skin simulant was constructed to study the incidence of friction blisters. The skin simulant consists of a thin polyurethane top layer and textured gum foam rubber bottom layer adhered to an acrylic backing plate to emulate the layered structure of the human skin. Friction blisters were produced on the skin simulant by using a dual axis tribometer. The effect of the applied normal load on the number of cycles required to produce a blister was investigated. The skin simulant was also analyzed as an adhesive bonded laminar composite to determine the relationship between the applied normal load and the number of cycles for blistering. The normal load and the number of cycles were found to be inversely related and vary by a power law function, as observed in previous work on human subjects in Naylor's pioneering study. The results obtained from the experimental data and the fracture mechanics modeling of the skin simulant indicate the potential of elastomeric skin simulant in providing useful insight into blister mechanics and other tribological properties of skin.

2.1 Introduction

Skin is the largest organ in the human body, and is the body's first line of defense against damage and infection. Friction blisters are one of the most common forms of damage that occur

to human skin. Friction blisters usually cause mild discomfort but can be a major cause of concern when they lead to intense pain, cellulitis and sepsis. They can compromise performance in athletes and military personnel. In a study where soldiers participated in a 20 km road march, 69% were found to have blisters and 10% of them had severe enough blisters to require medical intervention [1] . Blisters are also one of the three most important types of injuries in marathon runners [2]. The first significant effort towards studying skin friction blistering began with Naylor's experiments to study the effect of skin friction on load carrying for Army operational research. Naylor showed the existence of a parameter similar to coefficient of friction for the skin and that it depends on environmental conditions [3]. To better understand the mechanical properties of the skin, and analyze skin damage, like blisters, from a mechanical failure standpoint, it is important to have a basic idea about the structure of the skin.

Human skin is a complex system with two distinctive layers called the epidermis and the dermis, which are connected to the subcutaneous bone and muscle tissues through the hypodermis. The outermost layer, the epidermis, is in turn divided into five layers, outermost to innermost being the stratum corneum, the stratum lucidum, the stratum granulosum, the stratum spinosum and the stratum basale. The stratum basale is a layer of living cells, and it marks the transition from living cells in the dermis to dead cells in the epidermis. In his experiments on friction blistering, Naylor showed that when there is a sufficient friction force between the skin and the rubbing surface, blister formation occurs through an intra-epidermal split caused by prickle cell necrosis and filling of the split with blister fluid [4]. In his pioneering work with human subjects, Naylor also showed that there exists an inverse relationship between the number of rubs required to produce a blister and the frictional force. [4]. Two conditions were proposed to be critical for blister formation: 1) firm attachment of the lower epidermis to the adjacent

tissue, and 2) sufficient thickness of the stratum corneum. This may be one of the reasons that the most common occurrences of friction blisters are on palms and soles of the feet [5]. Research done on extensibility of the skin has shown that when the skin extends, three factors act consecutively: 1) convolutions in the dermal collagen fibers straighten out, 2) the dermal collagen fibers get aligned parallel to each other in the direction of the load, and 3) as the load increases, the aligned fibers extend. This phenomenon is responsible for directional variations in extensibility of the skin at various locations [6]. In this respect, skin behaves like a typical elastomer, and it suggests that elastomers can be used to model skin. So far, the study of friction blisters has been done primarily on human subjects. Friction blisters have also been successfully produced in animals to facilitate study on blisters without human subjects [7]. However, both of these methods are difficult due to current regulations on experiments with human and animal subjects, and because they also create huge variability in results due to variations in properties of the skin from subject to subject and from animals to humans. Recently, attempts have been made to characterize the blisters from an engineering standpoint by using a synthetic skin simulant platform, and blisters have been produced successfully under various conditions [8]. Using a synthetic simulant improved repeatability of the results and decreased variability across the sample.

It has been proposed by Comaish et al. that epidermal fatigue due to shear stress from the frictional force on the surface of the skin could be the cause of friction blistering [9]. In the current study, the authors focus on improving the aforementioned synthetic skin stimulant platform to study the effect of normal load on blistering. A fatigue based fracture model is proposed that models the skin simulant as an adhesive bonded laminar system to provide some insight into blistering mechanics. Also discussed are some of the current methods for

determining fatigue properties of laminar composites and their applicability to the skin simulant approach used in this work.

2.2 Materials and Methods

2.2.1 Skin simulant design and preparation

The skin simulant used in this study consists of two layers with an acrylic backing plate. The top layer simulates the epidermis and the bottom layer simulates dermis, fat and muscle tissue beneath the epidermis. Each of them will henceforth be referred to as epidermal simulant layer (ESL) and dermal simulant layer (DSL) respectively. The acrylic backing plate adhered to the DSL has a two-fold use. It simulates bone beneath the tissues, and it acts as support for the tribological testing purposes. Previous friction blistering studies on the synthetic skin simulant platform showed that the simulant experienced significant substrate effects during testing due to thinness and compliance of layers, and that it is imperative to use a support beneath layers during tribological testing [8].

The simulant was designed to replicate the blister formation mechanism of human skin, more specifically blisters formed on the palms and soles. In light of this, the design takes into consideration the factors that were shown to play a role in the blister formation during experiments on human subjects. The first factor considered was the coefficient of friction (CoF) of human skin. A challenge in this field of research is the fact that the friction coefficient of skin varies widely based on a multitude of factors such as anatomical location and hydration state. Masen et al. reported a range of CoF values from approximately 0.2 to 1.3 of skin rubbing against a stainless steel counterface [10]. It has also been shown that elastomers, like polyurethane, exhibit friction values against steel that fall well within this range. Friedrich et al.

reported on PUR composites with friction coefficients in dry sliding ranging from 0.2 to 0.52 [11]. The case for using PUR as a dermal simulant is further bolstered by the similarity with skin when rubbing against other materials, as well. For instance, PUR, when tested against wool exhibited similar coefficient of friction as the skin on the palms [12, 13], and Derler et al. showed that PUR exhibited only slightly higher CoF than skin against a number of reference materials [12]. Therefore, due to its commercial availability in a liquid-castable form, its transparency when cured, and its frictional similarities to skin, a polyurethane RTV resin was used for the epidermal simulant layer. The ESL was made of a polyurethane (PUR) layer of thickness of 0.6 mm, approximating the thickness of the epidermis in human skin [14]. Sufficient thickness of stratum corneum is known to be an important factor to produce friction blisters [5]. The PUR film was casted from a two-part urethane RTV mold-making system (TAP Plastics, San Leandro, California, USA). Once cured, the ESL is transparent and has a resulting durometer of approximately 60 Shore-D (approximate equivalent elastic modulus of 7.0 MPa). The DSL consists of textured natural gum foam rubber with adhesive backing and has a thickness of 6.2 mm (McMaster-Carr, Elmhurst, Illinois, USA) and an approximate elastic modulus of 240 kPa. The textured surface of the DSL was selected to better mimic the ridged surface of the dermis than a smooth layer as was employed in a previous version of the skin simulant concept. The adhesive backing of the DSL was stuck to the acrylic backing plate. The ESL is cast to form a 70-mm diameter circular film on top of an 80-mm square DSL and was allowed to cure at room temperature for 24 hrs. The PUR film was cast without any mold release and when completely cured, attached itself firmly to the textured surface of the DSL. Figure 2. shows the skin simulant specimen with a completely cured ESL layer. Since no adhesive was used in bonding the ESL

and the DSL, constant adhesive bond strength was maintained for all the specimens throughout the experiment.

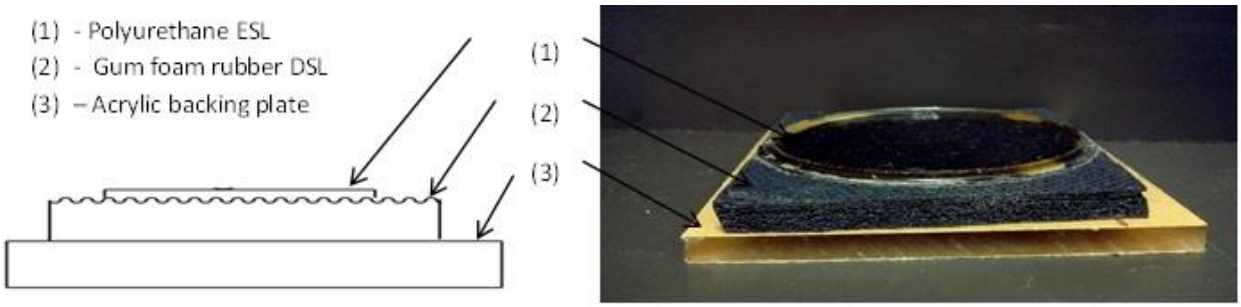

Figure 2.1 Synthetic skin simulant with different layers. The textured surface of the dermal simulant layer to emulate dermal ridges can be seen.

2.2.2 Blistering device

A dual axis tribometer was used to produce the blisters. The tribometer had a motion-controlled platform on which the specimen was firmly placed and had fixed stations to which a wear head was attached. The platform with the specimen reciprocated linearly under the stationary wear head. To enable blister formation without tearing the top layer on the thin-layered skin simulant, and to test the effect of the normal load over a wide range of loads, a low-weight station was specially constructed. This low-weight station used standard weights to apply normal load in the range of 3.11 to 5.56 N. Figure 2.2 shows the tribometer with the corresponding station used in the testing. The wear head used was an 18-8 stainless steel acorn nut (McMaster-Carr, “1/4 inch -20” thread, 11.1-mm width, 11.9-mm height). The diameter of the probe head was approximately 11.5 millimeters. Assuming a spherical head, and with the observation that the depth of penetration of the head was significantly greater than the thickness of the ESL, the range of predicted maximum contact stresses was from 130 to 155 kPa, using a Hertzian elastic model.

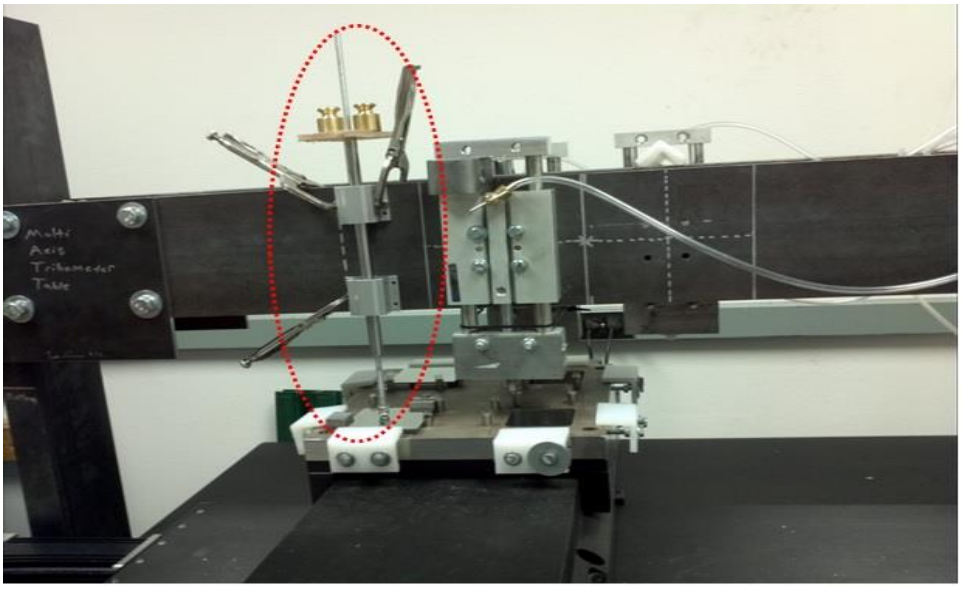

Figure 2.2 The dual axis tribometer with motion controlled platform and fixed stations. The low-weight station with standard weights used to apply normal load could be seen (dotted circle, left).

2.2.3 Experimental method

The effect of the normal load on the number of cycles taken to form a blister was tested. Other parameters that were known to affect the blister formation on human skin like the coefficient of friction, adhesion between the layers, thickness of the layers and the shear speed [4, 5, 8] were kept constant. Both the surface of the simulant and the surface of the wear head were unlubricated and untreated in any way throughout the experiment to maintain a constant coefficient of friction. Additionally, the ambient temperature during the test was controlled and monitored to be in the range of 23 ± 1°C. The length of travel of the wear head over the surface of the simulant was 60-mm per cycle. A constant crosshead speed of 20 mm/s was maintained throughout the experiment, with the exception of the very short decelerations and accelerations experienced at the ends of the reciprocated path when direction was changed. The numbers of cycles taken to produce a blister at a given normal load were measured. The experiment was started with no weights added to the station, with a corresponding normal load of 3.11 N. The trials were repeated with incremental increases in normal load of 0.25 N with each step. The

experiment was repeated until the upper limit on normal load was reached. The upper limit on the normal load was defined as the minimum load at which the outer layer of the simulant fails by tearing before any blister was formed. The blister formation was characterized by the appearance of an opaque oval with a distinctly raised surface along the length of the travel as shown in Figure 2.3. Due to the viscoelastic nature of the materials used, it is likely that some inelastic recovery occurred after a significant time post-test, thus blister height was not directly measured. The production of the blister was manually observed and the test was terminated for each sample once a clearly distinguishable blister was produced. The tribometer control software recorded the number of cycles at which the test was terminated. This yielded the number of cycles for blister formation in each trial. One simulant sample was used for a total of three test runs. Trial and error were employed with pilot samples to determine a minimum spacing of approximately 15 mm between affected areas. This spacing was sufficient to ensure that none of the individual tests were affected by previous tests using the same sample. One test run was conducted for each load setting, thus statistical variation in blistering behavior was not able to be determined in this study.

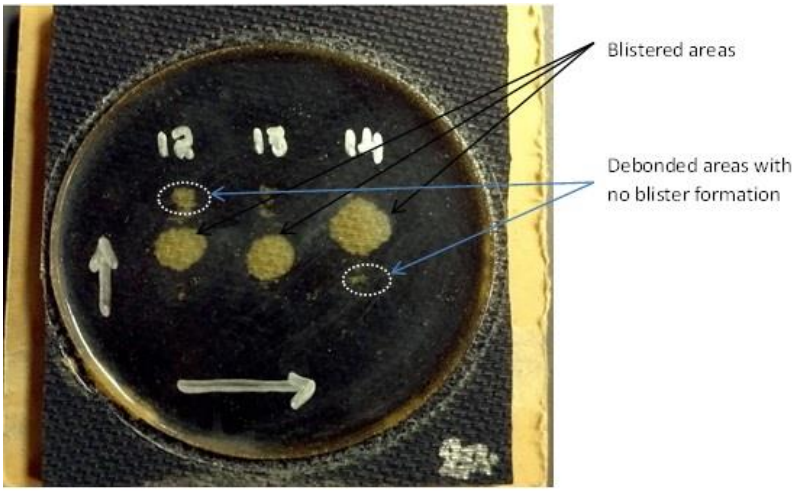

Figure 2.3 The skin simulant with blisters (larger opaque areas), from left to right formed at normal loads 3.85N, 4.09N, and 4.35N respectively. Also shown are the smaller debonded areas with no blistering (dotted circles).

2.2.4 Mechanical modeling of the skin simulant: relation between the normal load and the number of cycles

Fundamentally, the synthetic skin simulant is an adhesive bonded laminar system. The PUR in the ESL acts as an adherand as well as the adhesive joining the ESL and the DSL layers. The most common modes of failure in adhesive bonded joints are: cohesive, adhesive and substrate failure, respectively [15]. Separation of layers at either the inter-laminar or intra-laminar level is the result of such failures. For the current synthetic simulant, considering one of the layers acts as an adherand as well as the adhesive, it was hypothesized that a probable failure mode is adhesive failure (AF). In the AF mode, separation appears at the adhesive-adherand interface [16]. During the blistering experiments, the synthetic skin simulant was subjected to cyclic normal compressive and shear loads. One way to describe blister formation is as an adhesive delamination due to fatigue loading. In such a model, the blister appears due to crack propagation between the adhesive and one of the layers. Fabrication and material defects like cavities, inhomogeneities, improper curing, were shown to act as nucleation site for cracks in the polymer-based adhesive bonded laminar composite systems [17].

Fatigue failure in the adhesive bonded laminar interfaces is a complex phenomenon and there is no universally accepted criterion to explain it. However, assuming low numbers of fatigue cycles and a linearly elastic and isotropic system, linear elastic fracture mechanics (LEFM) techniques have been used in the past to evaluate the crack growth under fatigue loading and have made reasonable predictions for fatigue life [18]. The fatigue process is characterized by three stages: 1) crack initiation, 2) crack propagation, and 3) fast crack propagation [18]. A classic model by Paris suggested that the relationship between rate of crack growth and fracture

toughness follows a power law [19]. With reasonable estimates of initial crack length and stress intensity factor, the model can describe stage II crack propagation with reasonable accuracy [20].

The blisters formed on the synthetic skin simulant were oriented in the direction of motion of the wear head. Assuming a crack already exists due to fabrication defects or material inhomogeneities, the corresponding Paris model is

$$\frac{da}{dN} = C \cdot \Delta K_{II}^{m} \tag{1}$$

where *da/dN* is the rate of crack growth per loading cycle, *C* and *m* are empirical constants, and ΔK_{II} is the fluctuation in mode II (shear loading) stress intensity factor during the loading cycle. The top layer of the skin simulant was approximately 0.65 mm in thickness. Assuming a plane stress condition, the change in mode II stress intensity factor under a given fatigue loading is estimated by

$$\Delta K_{II} = 2\tau Y\sqrt{\pi a} \tag{2}$$

where *Y* is a dimensionless parameter whose value depends on the geometry of the specimen and the crack dimensions, and τ is the shear stress due to friction force. Y is assumed to be independent of crack length for short cracks. The stress intensity factor can be substituted in the power law equation and can be integrated to give number of cycles for failure thus yielding

$$N = \frac{2(a_f^{1-\frac{m}{2}} - a_i^{1-\frac{m}{2}})}{C(2-m)(2Y\sqrt{\pi})^m} \times \tau^{-m} \tag{3}$$

where a_f and a_i are the final and initial crack lengths respectively. This equation provides a means of predicting the number cycles required to produce a blister on the skin simulant based on applied normal load.

2.3 Results and Discussion

Blisters were formed under the given test conditions in all the trials at all normal loads. For each trial, during initial cycles of wear, as the wear head started to move long the surface of the skin simulant, the skin simulant was compressed in front of the wear head and was stretched behind it giving rise to a wave like disturbance across the surface of the skin simulant. This disturbance was similar to the "bow wave" observed by Kwiatkowska et al. during in-vivo testing on human skin rubbed against a reciprocating steel probe [21]. This was followed by the appearance of small opaque regions indicating localized debonding at the ESL-DSL interface. As the number of reciprocated cycles increased, the debonded regions extended along the length of the wear path, and coalesced to form a larger debonded region of the ESL. The debonded region of the ESL exhibited a wave like disturbance as the wear head reciprocated. This proceeded to form a blister with a distinctly raised opaque surface compared to the surrounding region of the ESL. However, not all of the debonded regions coalesced to form blisters, as can be seen in Figure 3. For all the trials, the blister formation occurred through this sequence of events as illustrated in Figure 4. For lower applied normal loads, all the above stages were clearly noticeable. These stages were similar to the blister formation stages of the Synthetic Skim Simulant Platform system by Guerra et al. [8]. As the applied normal load increased, the number of cycles required to form a blister drastically decreased.

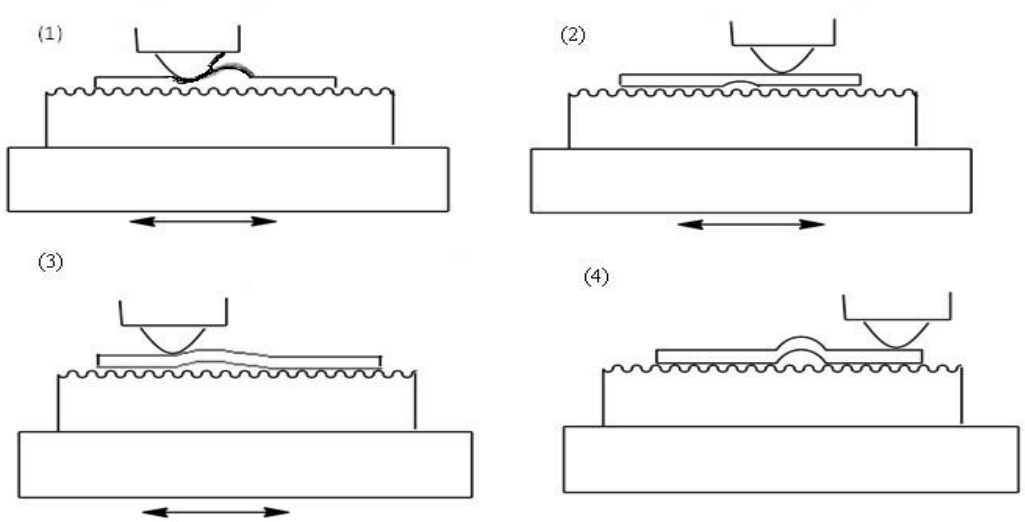

Figure 2.4 Illustration of the sequence of events leading to blister formation in the layered skin simulant. (1)As the wear head moves it compresses the surface of the skin simulant in front of it and stretches the skin simulant behind it forming a wave (2) Debonded regions appear at the ESL- DSL interface (3) Debonded regions grow and coalesce to form a large debonded zone along the length of the wear path. Debonded zone of the ESL exhibits a wave like disturbance (4) Formation of distinctly raised surface blister at which point experiment is terminated.

At higher normal loads, blisters formed before each of these stages could be individually observed for any appreciable amount of time. All the blisters formed were oval in shape and the major axis of the blisters formed is oriented in the direction of motion of the wear head. The position of the blister along the length of the wear path varied. Blister area was observed by visual inspection. While no noticeable pattern was found between the applied normal load and the position or the area of the blisters, there appeared to be an inverse relationship between the normal load applied and the number of cycles required to produce a blister, as shown in Figure 5. This is in accordance with Naylor's results from the blistering experiments on human skin [4]. There was a sudden drop in the number of cycles required to produce a blister, from the first trial with normal loading of 3.11 N to the next load incremental trial with normal load of 3.35 N. For the subsequent trials, the number of cycles required for blister formation decreased with the increasing normal load increments at a much slower rate. This could be due to an existence of a threshold with respect to the normal load required to produce a blister at the given set of

parameters for the skin simulant specimen (layer thickness, adhesion strength, cross-head speed and dermal stiffness).

Using the Paris model, debonding between the ESL and the DSL was analyzed as mode II delamination failure due to the interfacial shear stresses resulting from the tangential frictional force between the ESL and the wear head. In this approach, a constant coefficient of friction was assumed throughout the test as the surface texture and materials were held constant among all samples during the testing. As the normal load increased, the frictional force increased accordingly, as well as the shear stress experienced at the ESL-DSL interface. Hence, with increasing shear stress the number of cycles for failure decreased. Figure 2.5 shows the experimental data.

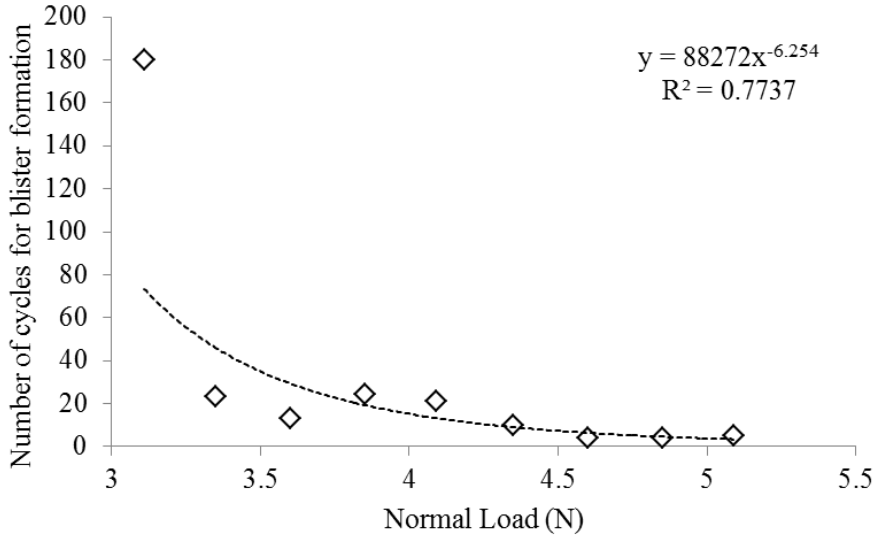

Figure 2.5 Curve showing the number of cycles required for blister formation as a power law function of the applied normal load, as fitted from the experimental data. Corresponding power law equation and the statistical parameter R^2 representing goodness of fit are also shown.

As shown, a Paris type power-law model was fit to the data to relate applied normal load to number of cycles required to produce a blister, yielding a least-squares fit of the form

$$N = 88300F^{-6.25} \tag{4}$$

The R-square value for the fit is 0.77 indicating the data are reasonably described by the crack propagation model (3). The degree of this correlation suggests that the mechanical aspects of friction blistering may indeed be tied to a fatigue mechanism in the ESL-DSL interface, analogous to the stratum basale.

The crack propagation model in this form did not take into consideration the effect of other important factors including shear speed, which undoubtedly affects viscoelastic systems such as skin. Also the assumptions of linearity and elasticity may not hold true through the entire process of crack propagation under cyclic loading. These issues can potentially be addressed by using the strain energy release rate parameter instead of a stress intensity factor, *K*. Modified crack growth models which use strain energy release rate have been used successfully to predict fatigue life of adhesive bonded systems such as the simulant used here [18]. Such models are generally of the form:

$$\frac{da}{dN} = C_i \cdot \Delta G^n \tag{5}$$

where ΔG is the change in strain energy release rate [17], while C_i and n are empirical constants. However, the value of n is smaller than that of m. The strain energy release rate parameter, G, takes into consideration mean stress along with change in stress state, as mean stress is known to influence crack growth. G and K are related by:

$$\Delta G = \frac{K_{\max}^2 - K_{\min}^2}{E} \tag{6}$$

where E is the elastic or flexural modulus of the adhesive [22]. Standard test configurations like the End Notched Flexure (ENF), the End Loaded Split (ELS) and the Four-Point End Notched Flexure (4ENF) have been used for studying the fracture in pure mode II and determining the

strain energy release rate parameter, G. Finite element analysis has also been proposed to find the value of the parameter using methods like the virtual crack closure technique [23]. Such modeling of the skin simulant, as well as actual skin, may give an estimate of the sensitivity of the debond growth rate with respect to applied normal load [17]. Using the strain energy release rate approach might also provide better insight into the reasons why only certain debonded regions became blisters in this investigation, thus giving further insight into blister mechanics. The ability to model this system from a fracture mechanics perspective may also increase the general applicability of the skin simulant to study other means of mechanical skin damage.

Future investigation employing this skin simulant approach is required in order to address limitations of the current study. Though it was beyond the scope of this study, failure mode analysis may be conducted in future work to better understand the debonding mechanism observed here. The simulant approach used here assumes that the CoF was constant throughout the wear cycle and as cycles were accumulated. Because of sweat, inflammation and temperature rise, it is known that the friction coefficient may change drastically before blister onset. Better characterization of the existence of a normal load threshold needs to be investigated by studying its dependence on other parameters such as layer thickness and inter-layer adhesion strength. Dermal ridges are known to affect the mechanical properties of the skin; however, the effect of dermal ridges on blistering is not known at this point. Also, the effect of other parameters like dermal stiffness and sliding speed needs to be further investigated over a wider range of normal loads. While the existing experimental approach shows merit, addressing these additional issues may aid in making the synthetic skin simulant more robust in representing human skin for friction blistering research.

2.4 Conclusions

A two-layer elastomeric skin simulant was constructed to study the relationship between applied normal load and number of cycles required to produce blistering, analogous to Naylor's pioneering work with human subjects. The results were analyzed to determine if they behaved in a manner consistent with a fatigue-based crack-growth failure process. The following conclusions can be made from the results:

1. The normal load and the number of cycles for blister formation are inversely related. This is in accordance with the behavior of human skin during blister formation as previously reported by Naylor.
2. There appeared to be a threshold value of interfacial shear stress that was required to produce friction blisters in the simulant. This agrees with empirical observations in human subjects.
3. The ex vivo elastomeric simulant approach was shown to be a promising tool for investigating dermal injury phenomena, thus helping to avoid the challenges encountered in frictional injury studies with human subjects.
4. A fracture mechanics based crack growth model showed some agreement with the friction-induced blistering of this multi-layer elastomeric system. This suggests that further investigation may be in order to determine if dermal blistering can be described as a crack-growth process.

2.5 References

[1] Brennan, F.H.J. Managing Blisters in Competitive Athletes. Current Sports Medicine Reports 1:319-322 (2002).

[2] Jaworski, C.A. Medical Concerns of Marathons. Current Sports Medicine Reports 4:137-143 110.1097/1001.CSMR.0000306196.0000351994.0000306195f (2005).

[3] Naylor, P.F.D. The Skin Surface And Friction. British Journal of Dermatology 67:239-248 (1955).

[4] Naylor, P.F.D. Experimental Friction Blisters. British Journal of Dermatology 67:327-342 (1955).

[5] Sulzberger, M.B., Cortese Jr, T.A., Fishman, L., Wiley, H.S., Peyakovich, P.S. Studies on Blisters Produced by Friction. The Journal of Investigative Dermatology 47:456-465 (1966).

[6] Stark, H.L. Directional variations in the extensibility of human skin. British Journal of Plastic Surgery 30:105-114 (1977).

[7] Cortese Jr, T.A., Griffin, T.B., Layton, L.L., Hutsell, T.C. Experimental Friction Blisters in Macaque Monkeys1. The Journal of Investigative Dermatology 53:172-177 (1969).

[8] Guerra, C., Schwartz, C.J. Development of a Synthetic Skin Simulant Platform for the Investigation of Dermal Blistering Mechanics. Tribology Letters 44:223-228 (2011).

[9] Comaish, J.S. Epidermal Fatigue As A Cause Of Friction Blisters. The Lancet 301:81-83 (1973).

[10] Masen, M.A., Veijgen, N.K., Wolda, T., van der Heide, E.: Parameters Influencing the Friction of In Vivo Human Skin. Fifth World Tribology Congress. Place (2013)

[11] Friedrich, K.: Friction and wear of polymer composites / Klaus Friedrich. Düsseldorf : VDI-Verlag, Düsseldorf (1984)

[12] Derler, S., Schrade, U., Gerhardt, L.C. Tribology of human skin and mechanical skin equivalents in contact with textiles. Wear 263:1112-1116 (2007).

[13] Ramalho, A., Szekeres, P., Fernandes, E. Friction and tactile perception of textile fabrics. Tribology International 63:29-33 (2013).

[14] Lee, Y.L., Hwang, K.H. Skin thickness of Korean adults. Surgical and Radiologic Anatomy 24:183-189 (2002).

[15] Guan, Z.-d., Wu, A.-g., Wang, J. Study on ASTM Shear-loaded Adhesive Lap Joints. Chinese Journal of Aeronautics 17:79-86 (2004).

[16] Experimental and Numerical Failure Analysis of Adhesive Composite Joints. International Journal of Aerospace Engineering 2012:10 (2012).

[17] de Goeij, W.C., van Tooren, M.J.L., Beukers, A. Composite adhesive joints under cyclic loading. Materials & Design 20:213-221 (1999).

[18] Qiao, P., Hu, G. Mode-II Fatigue Fracture of Wood-Composite Bonded Interfaces. Journal of Composite Materials 38:453-473 (2004).

[19] Paris, P.C. A rational analytic theory of fatigue. Trends Engin 13:9-14 (1961).

[20] Pugno, N., Ciavarella, M., Cornetti, P., Carpinteri, A. A generalized Paris' law for fatigue crack growth. Journal of the Mechanics and Physics of Solids 54:1333-1349 (2006).

[21] Kwiatkowska, M., Franklin, S.E., Hendriks, C.P., Kwiatkowski, K. Friction and deformation behaviour of human skin. Wear 267:1264-1273 (2009).

[22] Ward, I.M.: Mechanical properties of solid polymers. Wiley, New York (1983)

[23] Rybicki, E.F., Kanninen, M.F. A finite element calculation of stress intensity factors by a modified crack closure integral. Engineering Fracture Mechanics 9:931-938 (1977).

CHAPTER 3. TACTILE DISCRIMINATION OF RANDOMLY TEXTURED SURFACES: EFFECT OF FRICTION AND SURFACE PARAMETERS

A paper submitted to the journal Biotribology.

G.P. Chimata and C.J. Schwartz

Abstract

The tactile discrimination sensitivity for fine randomly textured surfaces was evaluated and its relation to the surface parameters and the coefficient of friction was investigated. Discrimination tasks were performed using a two-alternative forced choice technique and the mean probability of perceiving a difference was measured for pairwise combinations of six fine-grit abrasive papers. The surface roughness parameters of the abrasive papers were measured using a contact profilometer and scanning electron microscopy images helped observe the surface microstructure. The coefficient of friction for each of the abrasive papers against human finger was measured for two sliding orientation of the finger: an 'aligned' orientation along the length of the finger and a 'transverse' orientation perpendicular to the length of the finger. Possible cases of theoretical probabilities of perceiving a difference for a given pair of tactile samples were proposed and the experimental probabilities were discussed within this context. Based on the evidence in existing literature, three measurable properties were chosen to investigate possible correlation with the mean discrimination probability: root mean square roughness, mean spacing of the profile peaks, and the mean coefficient of friction. Experimental evidence suggests that of the three parameters investigated, differences in the mean spacing and

the mean friction coefficients were more indicative of the probability of perceiving difference between a pair of fine textured samples.

3.1 Introduction

Tactile perception is one of the five primary sensory functions, that enables humans to have interactions with their environmental stimuli and is the primary mode of written communication for visually challenged. One of the earliest notable contributions to understanding the sense of touch was made by Katz[1]. Multiple studies for understanding neurological, psychological and physical aspects of touch have since been conducted. The need to understand every aspect of sensory touch is growing with the increasing interest in applications like haptic performance of consumer electronics, improving the communication systems for the visually challenged, development of bionic robotic systems and, optimizing the tactile feel of everyday packaging materials.

Tactile perception of texture of a surface involves processing of information about its material properties and surface micro-geometry. Studies using human evaluation of multiple everyday surfaces showed that the tactile perceptual space was multidimensional [2-4]. Further, perception of a textured surface was correlated strongly to the rough/smooth and the soft/hard dimensions, and to a lesser extent to the sticky/slippery dimension[2, 5]. Of these three dimensions, rough/smooth dimension was the most extensively studied one from both neurophysiological and psychophysical standpoints. The focus had been on how the ‘perceived roughness’ depends on factors such as surface geometry of the stimuli tested, and the effect of the normal force [6, 7], identifying underlying neural codes and mechanoreceptors involved [8, 9]. Most of the early studies dealt with perceived roughness of relatively rougher surfaces with

element sizes of the order of several hundreds of microns [6-14], and spatial coding mechanisms were favored as responsible for the roughness perception at this scale[9, 12]. However, later studies with finer textures revealed the importance of vibrational cues in fine texture perception and discrimination, there by implying the involvement of temporal coding mechanisms and provided evidence for the duplex theory of texture perception [15]. Involvement of vibrotactile cues in fine texture perceptions intuitively points to the involvement of friction too. Subjects were known to adjust friction and normal forces optimally during tactile exploration of surfaces based on topography of the surface[16]. However, the exact role of friction in tactile perception is still not very clear.

Discriminatory touch of textured surfaces was not as well investigated as roughness perception, and even those studies that did involve discrimination tasks were limited to subjective ranking of perceived roughness [17, 18]. Due to this reason, perceptual dimensions of texture discrimination apart from roughness may not come into play and, the factors influencing discriminatory touch would be same as those for the perceived roughness in such a case. Instead of identifying factors that influence the estimates of perceived roughness of textured surfaces, if the measurable gross physical attributes (such as surface roughness and friction) could be linked to perceptual attributes (such as the probability of differentiating between surfaces) in a discrimination task, it provides a means for quantitatively measuring the tactile discriminability of textures. And such a measure of tactile discriminability could be valid for a wide range of surfaces with varied roughness, hardness and stickiness properties.

In the current study, the tactile discrimination sensitivity of randomly textured surfaces was measured as the probability of discriminating between given abrasive paper pair using a

psychophysical experiment. The results were compared with the measured physical attributes like root mean square roughness of the surface, mean spacing between profile peaks of the surface and the coefficient of friction, to find a possible correlation. Abrasive paper stimuli were used as the randomly textured surfaces. Use of these natural stimuli enables changing topographical features without affecting other known dimensions of texture perception like hardness and stickiness by simply varying the grit sizes.

3.2 Experimental Methods

3.2.1 Tactile discrimination sensitivity measurement

3.2.1.1 Stimuli

The stimuli used were FEPA P-grit abrasive papers of grit sizes 2500, 2000, 1500, 1200, 1000 and 800. The corresponding mean grain sizes according to the FEPA standards were 8.4, 10.3, 12.6, 15.3, 18.3 and 21.8 μm respectively. Table lists the surface properties of the abrasive papers with their corresponding standard errors of the mean (SE) measured using a contact profilometer (Mahr, MarSurf SD26). The stylus tip of the profilometer was slid along three directions (two mutually perpendicular directions and one at a 45° angle to either of those directions) on the surface of the abrasive papers. The surface height data thus obtained was used to compute the autocorrelation function and the correlation lengths. Analysis of variance of the correlation lengths in different directions for each of the abrasive papers indicated that surface topography was random isotropic in nature. Scanning electron microscopy images of the abrasive papers (obtained by FEI Quanta 250 Field emission scanning electron microscope (SEM)) were obtained to compare the particle sizes with the standards. SEM images indicate that the maximum particle sizes were in accordance with the standard sizes provided by the

manufacturer (Figure 3.1**)**. For the tactile discrimination sensitivity experiment, the abrasive papers were cut into 78 × 90 mm sheets and attached with a double sided tape to 83 × 103 mm acrylic backing plates. Corresponding to 6 different abrasive papers, a total of 21 pairwise combinations of the stimuli were tested for each test subject. Fifteen of these pairs consisted of different grit sized samples, while six of them had samples with the same grit sizes.

Table 3.1 Surface Properties of abrasive papers

Grit	Average Roughness Ra(μm) ± SE	Root mean square roughness Rrms(μm) ± SE	Mean spacing of profile peaks Rs(μm) ± SE
P800	6.00 ± 0.18	7.72 ± 0.20	105.68 ± 1.96
P1000	5.69 ± 0.15	7.16 ± 0.18	74.52 ± 2.44
P1200	4.22 ± 0.10	5.31 ± 0.13	73.52 ± 1.53
P1500	3.98 ± 0.085	5.11 ± 0.13	64.10 ± 2.98
P2000	3.64 ± 0.034	4.59 ± 0.059	64.38 ± 2.40
P2500	4.05 ± 0.062	5.05 ± 0.093	62.77 ± 2.65

All surface roughness parameters of the abrasive papers were measured using a contact profilometer (Mahr, MarSurf SD26), and the standard errors were calculated for 5 trials for each of the parameters. The sliding direction of the stylus tip was parallel to the grit number printing on the back of the abrasive papers for all the trials considered.

3.2.1.2 Subjects

For the tactile discrimination sensitivity experiment, a total of 26 subjects, 10 male and 16 female participated in the experiment. The participants were recruited based on their responses to the flyers posted at various locations across the university campus. All participants were above the age of 18. And, all of them were right-handed.

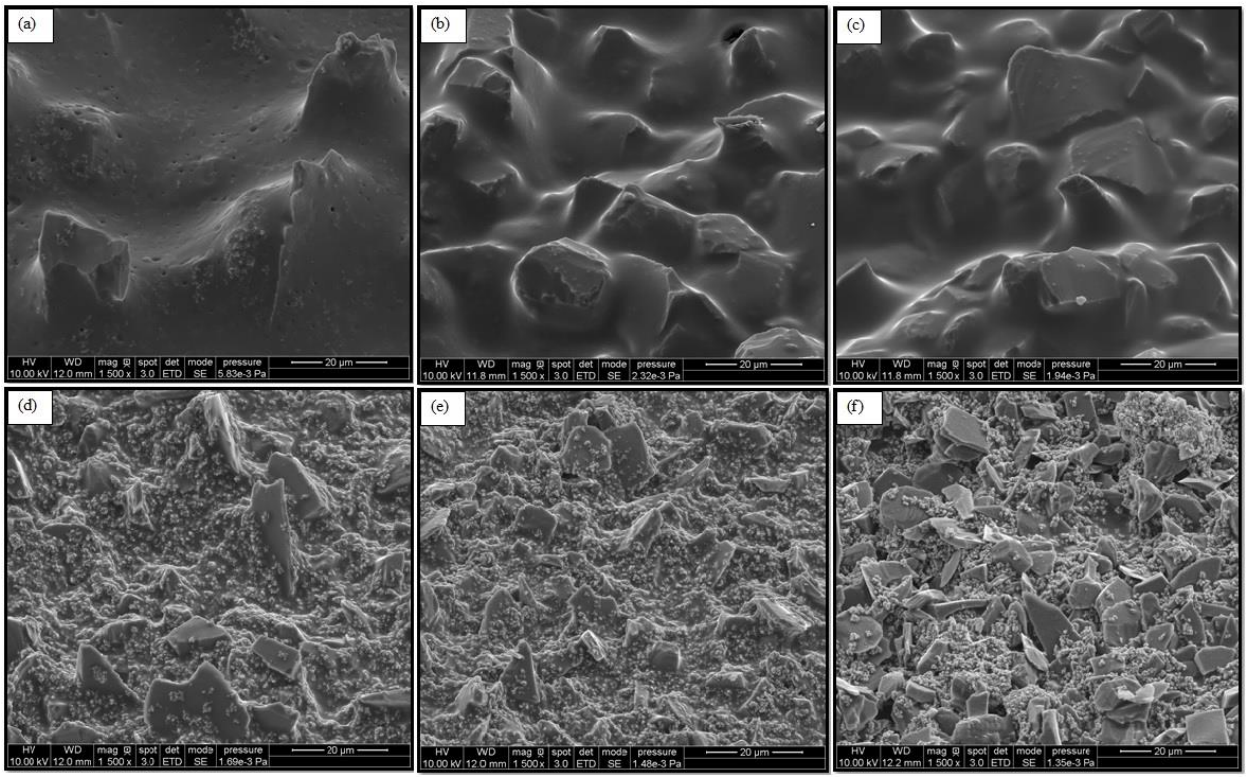

Figure 3.1 Scanning Electron Microscope images of abrasive papers (top left through bottom right) (a) P800, (b) P1000, (c) P1200, (d) P1500, (e) P2000, and (f) P2500. All images were secondary electron images obtained at 1500X and 45° tilt.

3.2.1.3 Experimental Procedure

At the beginning of the experiment, the experimental procedures were explained to the subjects, the informed consent was obtained and then, the subjects were asked to wash their hands thoroughly with soap to prevent transfer of substances like oil and dirt from the hands on to the stimuli. The subjects were instructed to wipe their hands periodically during the experiment to prevent transfer of wear particles between the abrasive papers. The subjects were seated at a table, separated from the researcher by an opaque screen with a curtained opening through which the subjects can access the test stimuli. The screen and the opening were designed to prevent the subjects from receiving any form of visual input regarding the stimuli. A two-alternative forced choice technique was used for testing. For each pairwise combination of the abrasive papers tested, the subjects were given the two abrasive samples one after the other, and

were asked to decide whether the stimuli felt same or different. The subjects were allowed to feel a sample as for long as they wanted and were allowed to go back and forth between the samples in a pair as many times as they wanted. The subjects were asked to use their dominant hand for the testing purposes, but were not instructed to use any specific finger for testing. Each of the 21 combinations tested were repeated 4 times per subject during each test, to give a total of 84 pairwise comparisons per test subject. The room temperature during testing was maintained at around 22 °C. The abrasive paper samples and the test set up can be seen in Figure 3.2.

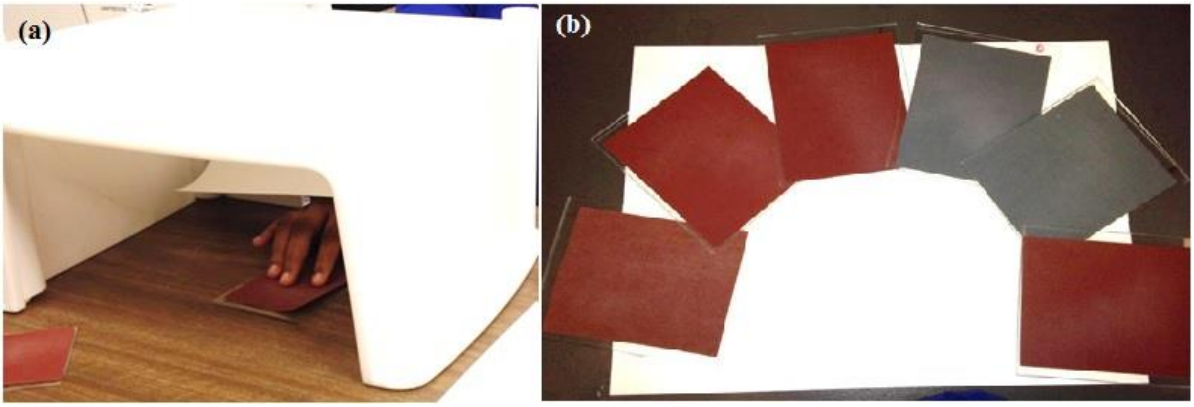

Figure 3.2 (a) Tactile Discrimination test setup as viewed from the experimenter's side. A subject's fingers probing a sandpaper sample can be seen. (b) Abrasive samples used for the test. Finest (P2500) to coarsest (P800) were arranged from left to right.

3.2.2 Friction measurement

3.2.2.1 Stimuli

The same six abrasive paper grits used for the tactile discrimination sensitivity experiment were also used for the friction measurements. Based on a preliminary test for the tactile perception experiment, it was observed by the participants and the researchers that sliding finger across abrasive papers felt different in different sliding orientations. In order to better understand and account for this directionality, for each abrasive paper, coefficient of friction was measured for two finger orientations, an aligned orientation and a transverse orientation. For the

aligned orientation, the length of the finger was in-line with the direction of motion of the finger, whereas for the transverse orientation, the length of the finger was perpendicular to the direction of motion of the finger. For the abrasive papers, the direction parallel to the grit number printing on their back was assigned as the sliding direction. And, for the friction measurements, the abrasive papers were cut into 65 X 20 mm strips along the sliding direction and were mounted on a 152 X 101 mm steel backing plates. The sliding direction for an abrasive paper and finger orientations can be seen in Figure 3.3.

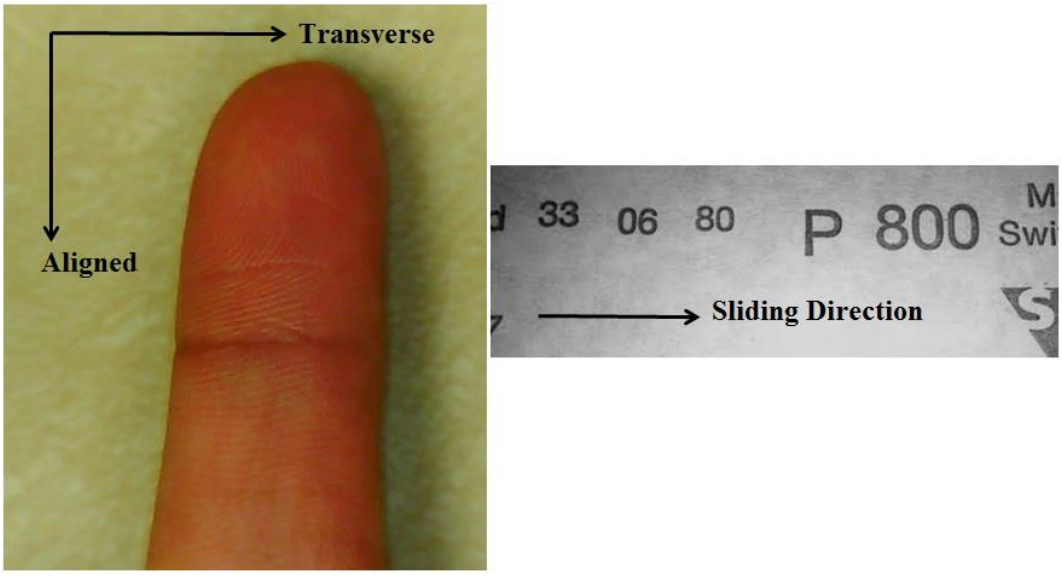

Figure 3.3 (a) The transverse and aligned finger sliding orientations with respect to the length of the finger (b) The sliding direction for P800 grit abrasive paper based on the printing on the back. The sliding direction was similarly assigned for all the six abrasive papers.

3.2.2.2 Experimental Procedure

To measure the coefficients of friction (COF) of the abrasive papers, one of researchers slid their finger along the length of the cut abrasive paper surfaces. Eleven trials were conducted for each abrasive paper, for each of the finger orientations. For all the measurements, the sliding angle between the surface and the finger was approximately between 30° and 45° and the sliding speed was maintained approximately between 0.8 cm/s and 1.2 cm/s. The normal load applied

was approximately 0.5 N. A three axis dynamometer (Kistler 9254), was used to measure the normal load applied and the resultant tangential friction force. A LabVIEW data acquisition program was used for data sampling at 1000 Hz. The coefficient of friction was calculated at each time step using Amonton's law and the average COF for each trial was computed using at least 1500 consecutive data points. The variation of the COF during each trial for all the 132 trials (eleven trails per abrasive paper per orientation for six abrasive papers and two orientations) was characterized by a median standard deviation of 0.03.

3.3 Results

3.3.1 Tactile discrimination sensitivity

The tactile discrimination sensitivity experiment was performed to determine the probability with which a participant was able to discriminate between any given two abrasive papers of the six abrasive papers tested. A generalized linear mixed model (GLMM) was fit to the participant response data from the tactile discrimination sensitivity test using GLIMMIX procedure in SAS (Statistical Analysis System) software. This was done to take into account the variability among the test subjects along with the variability within a subject. This procedure assumed normal random effects among the participants, and the data was assumed to have a binomial distribution conditional to those random effects. From the GLLM, the mean probability of discriminating between surfaces in an abrasive paper pair and the corresponding standard errors were obtained (Figure 3.4). It has to be noted that for each pair of abrasive papers, the probability with which a participant perceives a difference was measured, but not whether the participant was correctly discriminating the pair. The difference is explained in detail in the following sections.

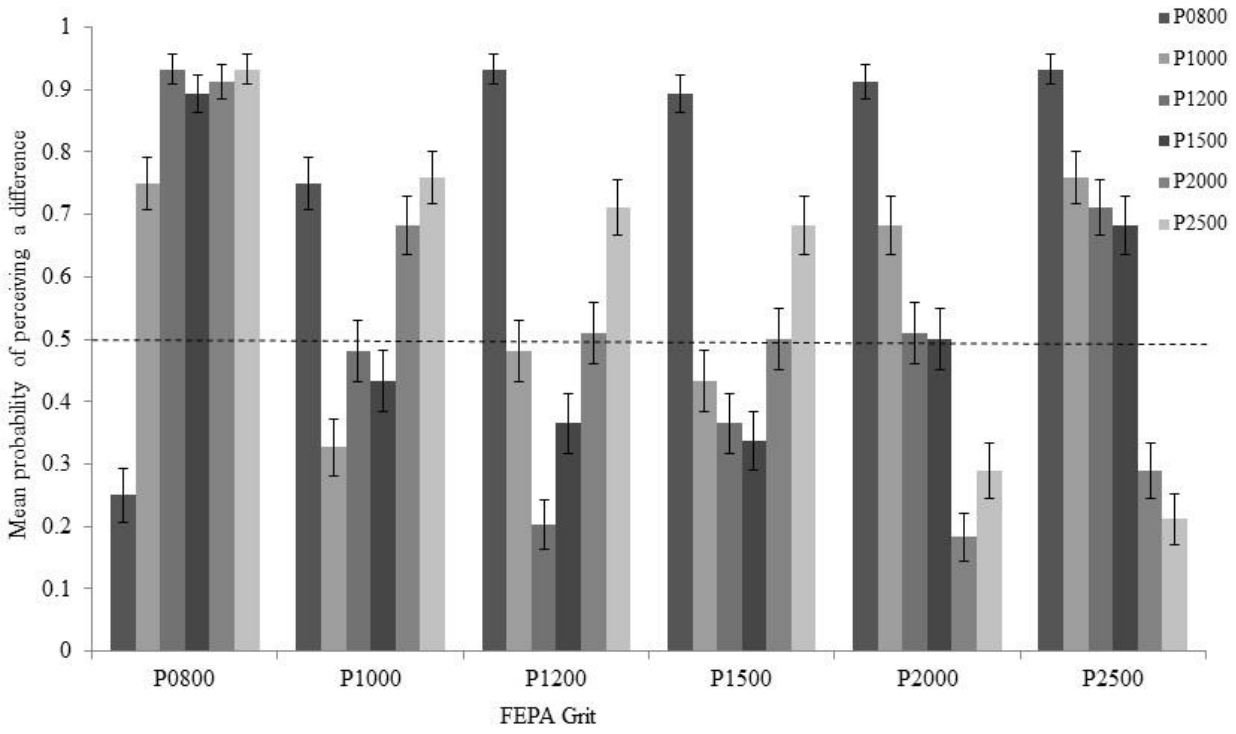

Figure 3.4 Mean probability of perceiving a difference between the abrasive paper grits with respect to different abrasive papers. Dashed line at p=0.5 indicates the probability of perceiving a difference when random choice is made in discriminating the abrasive papers.

To understand the empirical probabilities of discrimination ability of individuals, potential theoretical probabilities of discriminating between different combinations of grit pairs were proposed case by case and how the empirical probabilities fit into these scenarios is discussed.

Case 1: Perceptually unbiased

If a person was perceptually *unbiased*, i.e., the person had no sense of perception for discriminating between the given two surfaces, and if asked to make a judgment regarding difference between two grits, the person could have chosen to answer that they were same or different randomly. The possible outcomes of such a random choice experiment were:

A. The same grit pairs were identified as same.

B. The same grit pairs were identified as different.

C. The different grit pairs were identified as different.

D. The different grit pairs were identified as same.

Out of these four cases, A and C indicate correct discrimination of the grits and they can be classified as 'hits'. B and D lead to failure in discriminating the grits. B can be classified as a 'false positive' and D as a 'miss' in perceiving the difference between the grits.

Only two of the cases, B and C, lead to perceiving a difference. Therefore, the theoretical probability of perceiving a difference by making a purely random choice in discriminating the grits is $p = 0.5$.

Case 2: Bias towards perceiving a difference and reliable discrimination for different grit pairs

If a person *always* reported a difference between any given two grits, then he/she perceived both the same grit pairs and the different grit pairs as being different. This scenario leads to a theoretical probability of perceiving a difference of $p=1$. This could be considered as a case of biased random choice experiment where the person making the judgment was biased towards perceiving a difference all the times i.e., a 100% bias.

For the reliable discrimination of different grit pairs, a person was *biased* towards identifying different grit pairs as being different by means of their perceptual capacity. The empirical probabilities p in that case were $0.5 < p \leq 1$. The greater was the perceptual capacity of the individual, the greater was the bias towards correctly perceiving different grit pairs as different, and more did the probability of perceiving a difference tended towards 1.

For the nine different grit pairs (800 vs all other grits, 1000 vs 2000 and 2500, 1200 vs 2500, 1500 vs 2500), the mean probabilities of perceiving a difference from the experimental data were greater than 0.5 but less than 1. However, the mean probabilities of perceiving a difference were much higher for the pairs with 800 grit (800 vs all the grits) than for the rest of the pairs (1000 vs 2000 and 2500, 1200 vs 2500, 1500 vs 2500). This indicates there was a greater bias for decisions regarding certain pairs than for the others.

Case 3: Inability to perceive a difference and reliable discrimination for same grit pairs

If a person *never* detected the difference between any two given grits, then he/she identified both the same grit pairs and the different grit pairs as being same. This leads to the probability of perceiving a difference of exactly $p=0$. This could be considered a case of biased random choice experiment where the person making the judgment was biased towards never perceiving a difference i.e., a 100% bias.

For the reliable discrimination of same grit pairs, a person was *biased* towards identifying same grit pairs as being same by means of their perceptual capacity. The empirical probabilities p in that case were $0 \leq p < 0.5$. The greater was the perceptual capacity of the individual, the greater was the bias towards never perceiving a difference for a same grit pair, and more did the probability of perceiving a difference tended towards 0.

For the six same grit pairs (800 vs 800, 1000 vs 1000, 1200 vs 1200, 1500 vs 1500, 2000 vs 2000, 2500 vs 2500), the mean probabilities of perceiving a difference from the experimental data, albeit being low were never equal to 0. This deviation from the hypothesized minimum value indicates that the participants were usually but not always able to correctly perceive that there was no difference between the grits in same pair combinations.

For the three different grit pairs (1000 vs 1500, 1200 vs 1500, 2000 vs 2500) the mean probability of perceiving a difference was less than that of the random choice, and was particularly low for the grit pair 2000 vs 2500. This indicates a bias towards identifying the different grits in these pairs as being the same.

For the rest of the pairs (1000 vs 1200, 1200 vs 2000, 1500 vs 2000), the probabilities of perceiving a difference tended more towards a random choice than towards a particular bias. It was hypothesized that the differences in friction properties and/or measures of topographical features like average roughness and mean spacing between profile peaks affect the perceptual capacity. This perceptual capacity in turn determines the degree of the biases leading to a perceptual discrimination decision regarding textures. Each of these hypotheses is discussed in detail in subsequent sections.

In summary, the coarsest grit (P800) and the finest grit (P2500) were most certainly discriminated from all the other grits. Exception being the case of P2500 vs P2000 grits and it was the only case where one grit was discriminated from the other with a probability as low as that of a same grit-pair comparison. Even though the P2000 grit was perceived to be same as the P2500 grit, it was not as well discriminated from the other grits as the P2500 grit. If the grits were to be categorized based on the average ability of the individuals to clearly discriminate between the categories, the grit tested fell into three groups, P800 in the first group G1, (P1000, P1200, P1500) in the second group G2 and (P2500, P2000) in the third group G3.

3.3.2 Friction measurement

The coefficient of friction of the abrasive papers when rubbed against the skin on the finger pad, was measured in two finger sliding orientations (aligned and transverse), to determine

the correlation, if any between the finger pad friction and the tactile discrimination sensitivity. The variation of the coefficient of friction of the abrasive paper grits was different for the aligned and the transverse orientations (Figures 3.5 – 3.7). Also, no linear correlation was seen between the coefficients of friction and the surface properties (mean particle size, root mean square roughness or the mean spacing between the profile peaks) of the abrasive papers for the grits tested.

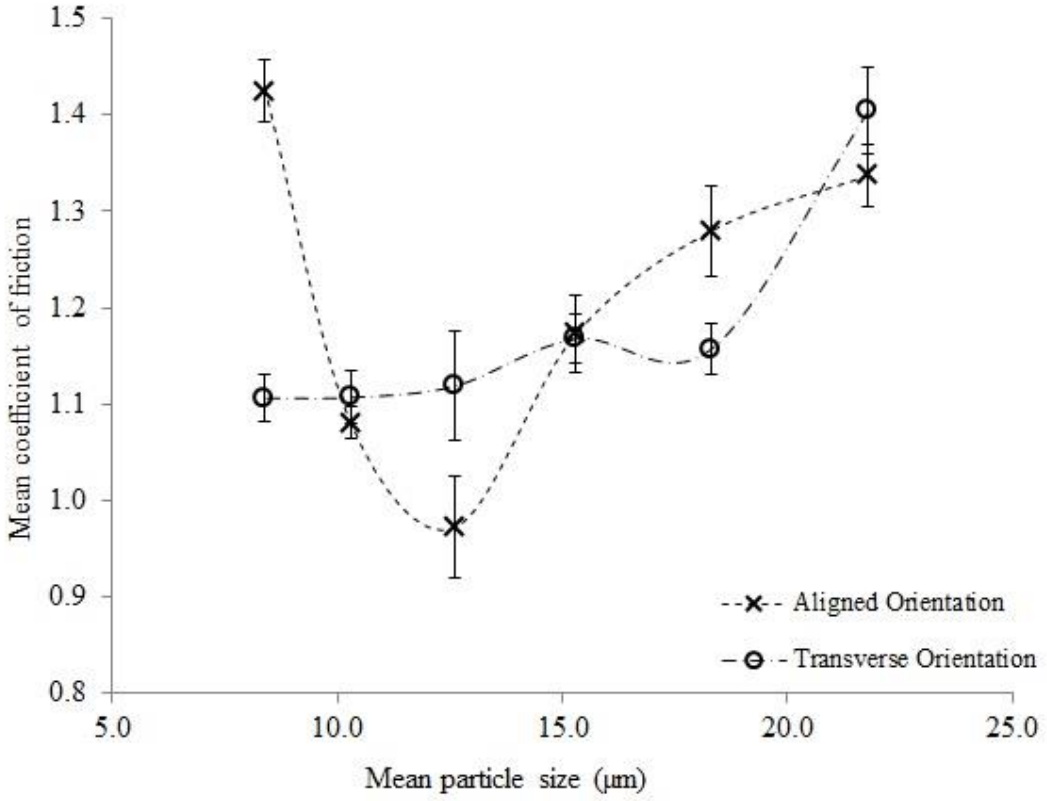

Figure 3.5 Variation of the mean coefficient of friction with the mean particle size of the abrasive papers (finest to coarsest) in the aligned and the transverse orientations. The mean particle sizes for the grits P2500 through P800 were 8.4, 10.3, 12.6, 15.3, 18.3 and 21.8 μm respectively.

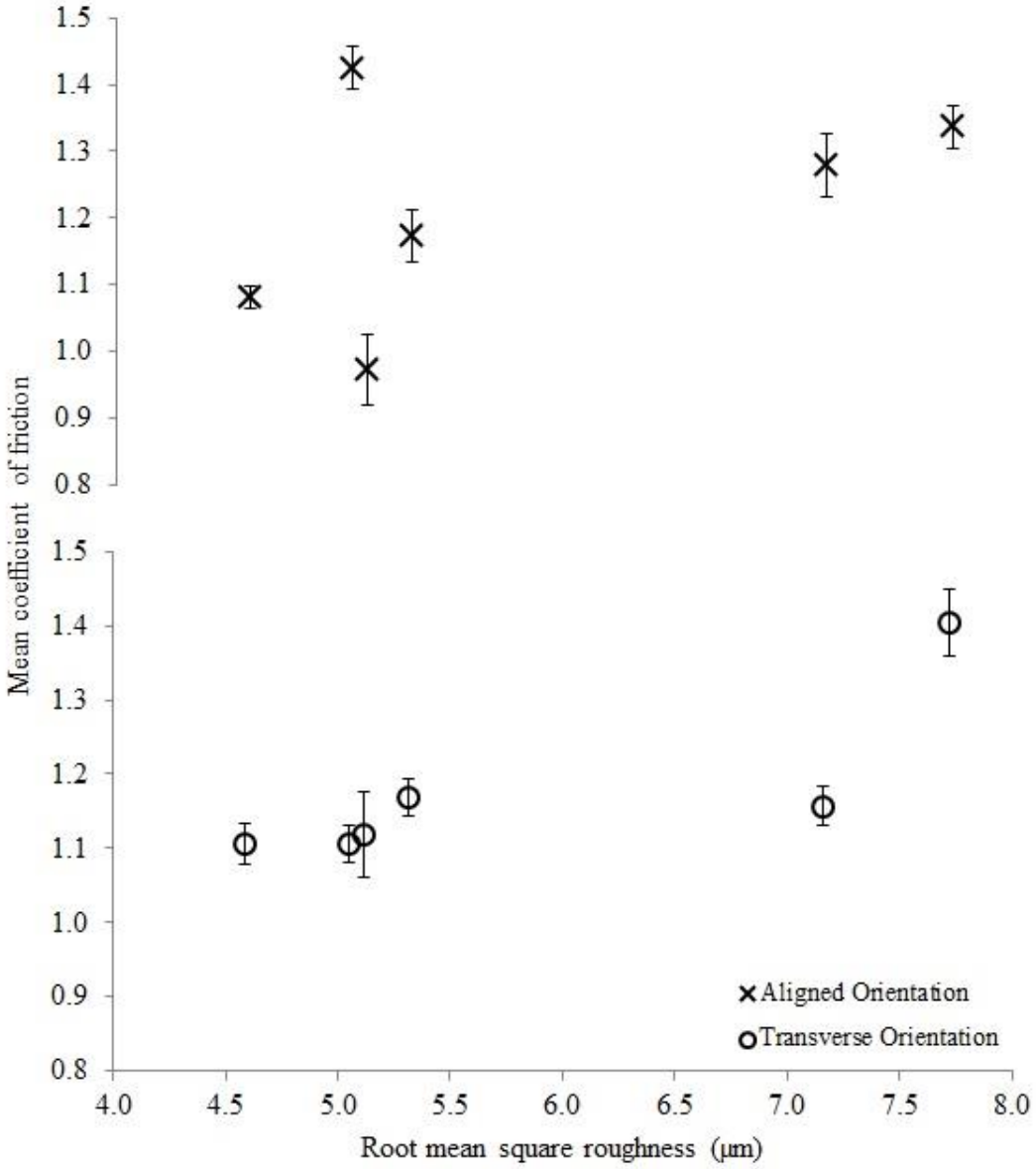

Figure 3.6 Variation of mean coefficient of friction with the root mean square roughness of the abrasive papers in the aligned and transverse orientations

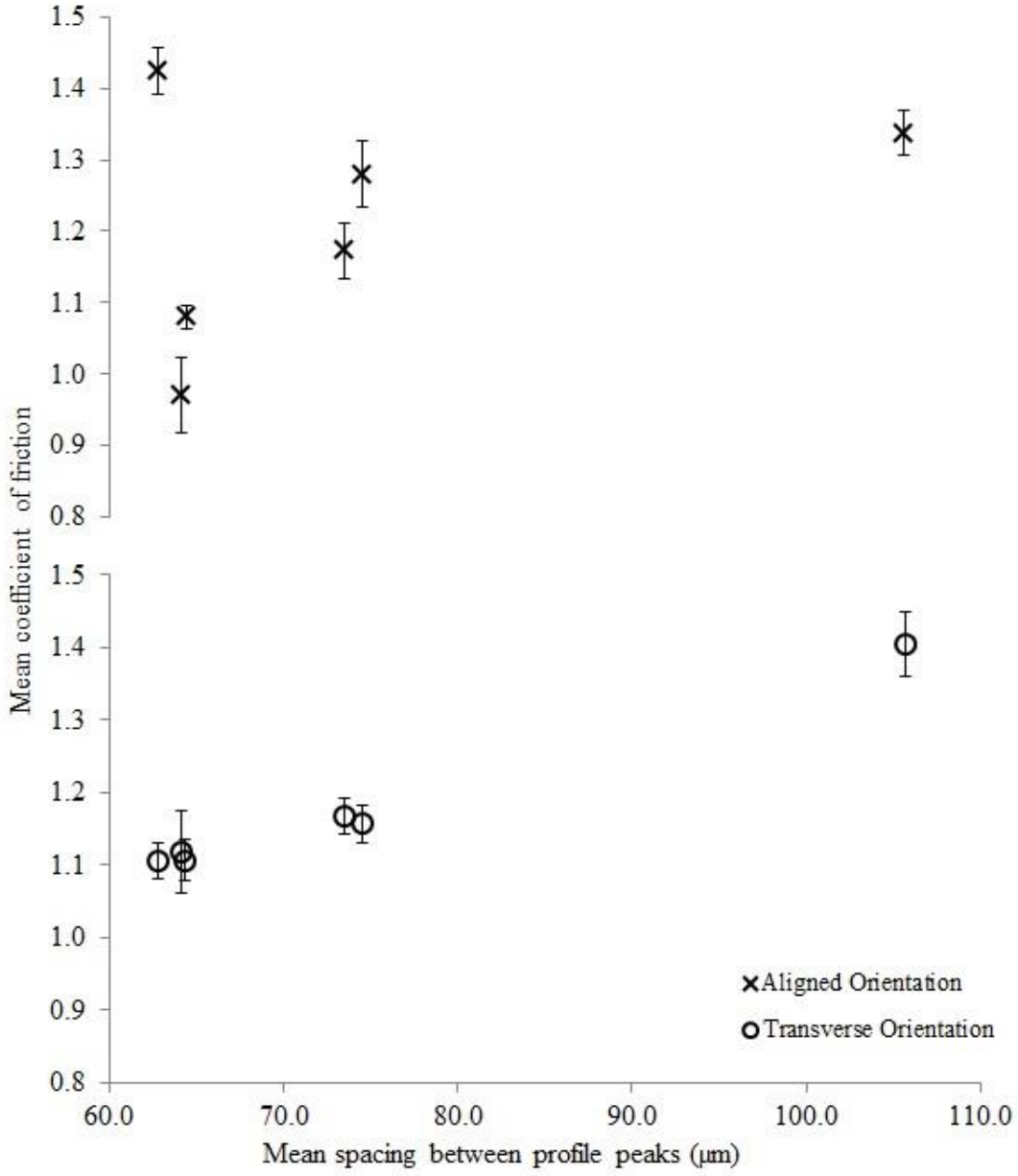

Figure 3.7 Variation of mean coefficient of friction with the mean spacing between profile peaks of the abrasive papers in the aligned and transverse orientations.

In the aligned orientation, the coefficient of friction for the P2500 (finest) grit was the highest, followed by a decrease in the COF leading to a minimum for the P1500 grit, and then an increase reaching a maximum again for the P800 grit. The COF values for the P800 and P2500 grits were quite close. Similar trend in the coefficient of friction in the aligned orientation was

observed with the increase in mean spacing of profile peaks. At the lowest spacing there was a high COF, followed by a sharp decrease in COF with increasing spacing reaching a minimum and then a sharp increase which plateaued off. However, no clear trend could be seen in the variation of the coefficient of friction with the root mean square roughness, especially at lower roughness values.

In the transverse orientation, the COF value for the P2500 grit was the lowest, followed by a slow increase in the COF up to P1200 grit, and then a slight decrease at P1000 grit followed by a sharp increase reaching a maximum at P800 grit. With the increasing root mean square roughness Rrms, similar trend in the coefficient of friction was observed. However, with the increasing mean spacing Rs, the COF values increased consistently. It was believed that COF for the abrasive papers tested was a summation of adhesion, hysteresis and interlocking components of friction. The dominant mechanism of friction acting for each grit combined with the effect of topographical features of a finger like the fingerprints and the elastic property of the fingertip material led to these particular trends in the coefficient of friction. A detailed discussion of the friction mechanisms and the effect of surface features and elastic properties of finger is available elsewhere[19], and is beyond the scope of the discussion here.

3.4 Discussion

From multiple studies on roughness perception using dot and grating patterns, spacial distribution of the elements (dot or groove spacing) was known to play a key role in roughness estimation[6-9, 13, 20, 21]. Previous studies on fine texture discrimination using abrasive paper stimuli suggested that amplitude information of stimuli surface unevenness might be key to texture discrimination [22]. Friction induced vibrational cues during fingertip scanning surfaces

were known to mediate roughness perception in fine texture discrimination tasks [15, 23-26]. Friction was suggested to be related to coarseness perception of paper samples[27]. A recent study suggested that the coefficient of friction and the wavelength of the wrinkles could be related to the perceptual dimensions involved in differentiating nanoscale wrinkled surfaces from blank surfaces [28]. With these factors in mind, three potential hypotheses were considered to determine the relation between the tactile discrimination sensitivity of the abrasive papers and their friction and surface properties. The surface and friction property data from the three distinctly discriminable grits, one from each of the groups G1, G2 and G3 based on the participant perception data, was considered to determine the validity of the proposed hypotheses. Three abrasive paper grits P800, P1200 and P2500 representative of the groups G1, G2 and G3 respectively were considered for this purpose.

Root mean square roughness hypothesis

The mean probability of perceiving a difference between the grits was related to the difference in root mean square roughness of the corresponding grits. This would be true if the amplitude information of the surface elements determines the perception of fine texture discrimination. Table 3.2 shows the differences, ratios and logarithm of ratios of the in root mean square roughness for the abrasive paper grits and their corresponding probabilities for being perceived as different.

Table 3.2 Comparison of the probability of discrimination between an abrasive paper pair with the corresponding difference in the root mean square roughness

Grit 1	Grit 2	Mean probability of perceiving a difference	Difference in Rrms(μm) (p-values)*	Ratio of Rrms (p-values)**	Logarithm of ratio of Rrms (p-values)***
P800	P1200	0.93	2.67[1] (<0.0001)	0.69 (<0.0001)	-0.37 (<0.0001)

Table 3.2 continued.

P800	P2500	0.93	2.41[1] (<0.0001)	0.65 (<0.0001)	-0.42 (<0.0001)
P1200	P2500	0.71	0.27[1] (0.4252)	0.95 (.0475)	-0.05 (0.0595)

[1] Standard error of the mean difference in Rrms= 0.21
[*] Null hypothesis is difference in Rrms between the grits is 0
[**] Null hypothesis is ratio of Rrms of the grits is 1
[***] Null hypothesis is logarithm of ratio of Rrms of the grits is 0

Not all the grits which were clearly perceived to be different have different roughness values. This was slightly surprising, considering previous work [15] which indicated that perceived coarseness was directly related to the roughness. However, perceived roughness, which may depend on vibrational cues, might not be reflected in the measure of roughness used here. These results suggest that differences in roughness cannot be considered a stand-alone factor to determine the perception of differences in texture between fine textured surfaces.

Mean profile peak spacing hypothesis

The mean probability of perceiving a difference between the grits was related to the difference in mean spacing of profile peaks of the corresponding grits. This would be true if the spacing information of dominant surface features plays key role in perceiving differences in fine textured surfaces. Table 3.3 shows the differences, ratios and logarithm of ratios of the mean spacing of profile peaks for the abrasive paper grits and their corresponding probabilities for being perceived as different.

Table 3.3 Comparison of the probability of discrimination between an abrasive paper pair with the corresponding difference in the spacial spacing

Grit 1	Grit 2	Mean probability of detecting a difference	Difference in Rs (p-values)[*]	Ratio of Rs (p-values)[**]	Logarithm of ratio of Rs (p-values)[***]
P800	P1200	0.93	42.91[1] (<0.0001)	0.70 (<0.0001)	-0.36 (<0.0001)

Table 3.3 continued.

P800	P2500	0.93	32.16[1] (<0.0001)	0.59 (<0.0001)	-0.52 (<0.0001)
P1200	P2500	0.71	10.78[1] (<0.001)	0.85 (<0.001)	-0.16 (0.002)

[1] Standard error of the mean difference in Rs = 2.97
[*] Null hypothesis is difference in Rs between the grits is 0
[**] Null hypothesis is ratio of Rs of the grits is 1
[***] Null hypothesis is logarithm of ratio of Rs of the grits is 0

The differences in the mean spacing of the profile peaks were not only significant for the distinctly differently perceived grits, but a positive correlation can be seen between the probabilities of perceiving a difference between the grits. The results supported the hypothesis that distributed distinct surface features even in randomly textured surface like abrasive paper grits were playing a key role in perception of differences in textures and their spacing difference could be used a predictive measure for perceivability of differences between fine textured surfaces.

Coefficient of friction hypothesis

The mean probability of perceiving a difference between the grits was related to difference in coefficient of friction of the corresponding grits in either of the orientations tested. This would be true if the friction information was indeed being used perceive the differences in the textures. Table 3.4 shows the differences, ratios and logarithm of ratios of the coefficients of friction for the abrasive paper grits and their corresponding probabilities for being perceived as different.

Presence of differences in the coefficients of friction in either of the orientations could be seen to positively correlate to perceiving differences between the grits. This strengthens the hypothesis. If being used as a stand-alone factor, the differences in the friction based on

orientation can lead to inherent confusion in making the decision of perceiving a difference between textures. However, the differences in friction in addition to differences in topographical feature measurements like spacing between the profile peaks could have been used in perception of differences in fine textures.

Table 3.4 Comparison of the probability of discrimination between an abrasive paper pair with the corresponding difference in the coefficient of friction

Grit 1	Grit 2	Mean probability of perceiving a difference	Difference in COF		Ratio of COF		Logarithm of ratio of COF	
			Aligned (p-value)*	Transverse (p-value)*	Aligned (p-value)**	Transverse (p-value)**	Aligned (p-value)***	Transverse (p-value)***
P800	P1200	0.93	0.16[1] (<0.001)	0.30[2] (<0.0001)	0.87 (<0.001)	0.85 (<0.001)	-0.14 (0.002)	-0.16 (<0.001)
P800	P2500	0.93	0.09[1] (0.2212)	0.24[2] (<0.0001)	1.04 (0.0708)	0.80 (<0.0001)	0.04 (0.0846)	-0.23 (<0.0001)
P1200	P2500	0.71	0.25[1] (<0.0001)	0.06[2] (0.4213)	0.83 (<0.0001)	1.06 (0.035)	-0.18 (<0.0001)	0.07 (0.036)

[1] Standard error of the mean difference in COF in aligned orientation = 0.052, [2] Standard error of the mean difference in COF in aligned orientation = 0.048
* Null hypothesis is difference in Rrms between the grits is 0
** Null hypothesis is ratio of Rrms of the grits is 1
*** Null hypothesis is logarithm of ratio of Rrms of the grits is 0

3.5 Conclusions

The current study investigates tactile discrimination sensitivity in randomly textured fine-grit abrasive papers and makes an attempt at identifying factors that lead to perceivability of differences in fine textured surfaces. The following conclusions can be made from the results of the study.

- In order to clearly perceive a difference between two fine textured surfaces, there should be significant difference in the measures of distributed distinct topographical features like mean spacing of the profile peaks and the coefficients of friction of the textured surfaces compared.
- Differences in the average roughness measures (like root mean square roughness) were not representative of the ability of individuals to discriminate between fine textured surfaces.

3.6 References

[1] Krueger, L.E. David Katz's Der Aufbau der Tastwelt (The world of touch): A synopsis. Perception & Psychophysics 7:337-341 (1970).

[2] Hollins, M., Bensmaïa, S., Karlof, K., Young, F. Individual differences in perceptual space for tactile textures: Evidence from multidimensional scaling. Perception & Psychophysics 62:1534-1544 (2000).

[3] Bergmann Tiest, W.M., Kappers, A.M.L. Analysis of haptic perception of materials by multidimensional scaling and physical measurements of roughness and compressibility. Acta Psychologica 121:1-20 (2006).

[4] Chen, X., Shao, F., Barnes, C., Childs, T., Henson, B. Exploring Relationships between Touch Perception and Surface Physical Properties. International Journal of Design 3 (2009).

[5] Holliins, M., Faldowski, R., Rao, S., Young, F. Perceptual dimensions of tactile surface texture: A multidimensional scaling analysis. Perception & Psychophysics 54:697-705 (1993).

[6] Lederman, S., Taylor, M. Fingertip force, surface geometry, and the perception of roughness by active touch. Perception & Psychophysics 12:401-408 (1972).

[7] Lederman, S.J. Tactile roughness of grooved surfaces: The touching process and effects of macro- and microsurface structure. Perception & Psychophysics 16:385-395 (1974).

[8] Connor, C.E., Hsiao, S.S., Phillips, J.R., Johnson, K.O. Tactile roughness: neural codes that account for psychophysical magnitude estimates. The Journal of Neuroscience 10:3823-3836 (1990).

[9] Connor, C.E., Johnson, K.O. Neural coding of tactile texture: comparison of spatial and temporal mechanisms for roughness perception. The Journal of Neuroscience 12:3414-3426 (1992).

[10] Stevens, S.S., Harris, J.R. The scaling of subjective roughness and smoothness. Journal of Experimental Psychology 64:489-494 (1962).

[11] Lederman, S. “ Improving one’s touch” … and more. Perception & Psychophysics 24:154-160 (1978).

[12] Lederman, S.J., Loomis, J.M., Williams, D.A. The role of vibration in the tactual perception of roughness. Perception & psychophysics 32:109 (1982).

[13] Lederman, S.J., Thorne, G., Jones, B. Perception of Texture by Vision and Touch: Multidimensionality and Intersensory Integration. Journal of Experimental Psychology: Human Perception and Performance 12:169-180 (1986).

[14] Taylor, M., Lederman, S. Tactile roughness of grooved surfaces: A model and the effect of friction. Perception & Psychophysics 17:23-36 (1975).

[15] Hollins, M., Risner, S.R. Evidence for the duplex theory of tactile texture perception. Perception & Psychophysics 62:695-705 (2000).

[16] Smith, A., Gosselin, G., Houde, B. Deployment of fingertip forces in tactile exploration. Exp Brain Res 147:209-218 (2002).

[17] Smith, A., Chapman, C., Deslandes, M., Langlais, J.-S., Thibodeau, M.-P. Role of friction and tangential force variation in the subjective scaling of tactile roughness. Exp Brain Res 144:211-223 (2002).

[18] Morley, J., Goodwin, A., Darian-Smith, I. Tactile discrimination of gratings. Exp Brain Res 49:291-299 (1983).

[19] Chimata, G.P., Schwartz, C.J. Investigation of friction mechanisms in finger pad sliding against surfaces of varying roughness. Biotribology 3:11-19 (2015).

[20] Johnson, K.O., Phillips, J.R. Tactile spatial resolution. I. Two-point discrimination, gap detection, grating resolution, and letter recognition. Journal of neurophysiology 46:1177-1192 (1981).

[21] Johnson, K.O. Neural mechanisms of tactual forms and texture perception. Annu Rev Neurosci 15:227-250 (1992).

[22] Miyaoka, T., Mano, T., Ohka, M. Mechanisms of fine-surface-texture discrimination in human tactile sensation. The journal of the acoustical society of America 105:2485-2492 (1999).

[23] Prevost, A., Scheibert, J., Debrégeas, G. Effect of fingerprints orientation on skin vibrations during tactile exploration of textured surfaces. Communicative & integrative biology 2:422 (2009).

[24] Scheibert, J., Leurent, S., Prevost, A., Debrégeas, G. The role of fingerprints in the coding of tactile information probed with a biomimetic sensor. Science (New York, NY) 323:1503 (2009).

[25] Wandersman, E., Candelier, R., Debrégeas, G., Prevost, A. Texture- induced modulations of friction force: the fingerprint effect. Physical review letters 107:164301 (2011).

[26] Fagiani, R., Massi, F., Chatelet, E., Berthier, Y., Akay, A. Tactile perception by friction induced vibrations. Tribology International 44:1100-1110 (2011).

[27] Skedung, L., Danerlöv, K., Olofsson, U., Michael Johannesson, C., Aikala, M., Kettle, J., et al. Tactile perception: Finger friction, surface roughness and perceived coarseness. Tribology International 44:505-512 (2011).

[28] Skedung, L., Arvidsson, M., Chung, J.Y., Stafford, C.M., Berglund, B., Rutland, M.W. Feeling Small: Exploring the Tactile Perception Limits. Sci Rep 3 (2013).

CHAPTER 4. INVESTIGATION OF FRICTION MECHANISMS IN FINGER PAD SLIDING AGAINST SURFACES OF VARYING ROUGHNESS

A paper published in the journal Biotribology.

G.P. Chimata and C.J. Schwartz

Abstract

Human finger pad friction and the effects of surface features on the fingerprint ridges, shape of the finger and the material properties of the finger were investigated. The friction coefficients for three fine-grit abrasive papers were measured to assess these effects. Four probing surfaces were used: human index finger pad, silicone replicas of the finger with and without fingerprints, and a smooth silicone sphere. Friction tests were performed at a constant normal load of 0.5 N in two probe orientations: normal and perpendicular to the orientation of the fingerprint ridges. Scanning electron microscopy of the abrasive papers was performed to examine their surface topography. Based on the trends in coefficients of friction, topography of the abrasive papers, surface features of the finger pad, and the shape and elastic properties of the finger, possible friction mechanisms were discussed. It was inferred that the change in the shape of the probe (from a sphere to the finger shape) changes the adhesion and deformation components of friction, presence of fingerprints adds an interlocking contribution to the friction and decrease the adhesion and deformation components of friction, and the elastic properties of the finger lead to an increase in all the three components of friction.

4.1 Introduction

Fingers play an important role in handling, manipulating, gripping and perceiving surfaces and objects during multiple everyday tasks. It was established that the friction between the fingers and an object is one of the factors that influences the grip force employed by individuals in precision grip activities like grasping and lifting objects[1]. During active tactile exploration of surfaces using fingertips, it was observed that the normal contact force and tangential shear force (friction force) were optimally adjusted depending on the topography of the surface being explored[2]. Therefore, it's evident that finger-surface friction is important for controlling all these interactions, and understanding the factors affecting finger pad friction can help in designing surfaces for improved efficiency in gripping, manipulation and perception tasks.

The coefficient of friction of a finger pad is not an intrinsic property of the skin and is dependent on the tribological system for which the measurement was made. The contact mechanics is influenced by the material and microgeometry of both the surfaces in contact, skin hydration, normal load and the relative velocity of the surfaces in contact. Finger pad friction properties were measured against a wide range of materials so far such as packaging materials[3], textiles[4, 5],metals[6-8], polymers[6, 8] and glass[9, 10] to name a few. The effect of the interacting surface's microgeometry on finger friction has been explored in studies on ridged surfaces with different ridge geometries to understand their effect on finger friction[7, 11]. Finger pad friction was used for comparing materials with skin like properties [4], designing artificial fingers[12, 13] and tactile attributes of textiles[5]. The effect of applied variables like normal force, sliding velocity and lubricants on finger pad friction has also been well characterized [6, 8, 14]. Inherent skin related phenomena like occlusion, sweating and the

sensitivity of coefficient of friction to these conditions were well investigated[9, 10]. More recently, Derler et al. identified ploughing and abrasion as important friction mechanisms during repetitive rubbing of fingerpad on abrasive surfaces[15].

Even with the existing research, the effects of surface features and the topography of the finger pad on the friction are not well characterized. Sliding a finger and a finger like sensor with ridges mimicking fingerprints across randomly textured surfaces induced oscillations in friction force of frequency that can be optimally received by the skin mechanoreceptors [16-18]. Further, it has been suggested previously that fingerprint ridges play a role in determining friction when interacting with ridged surfaces of dimensions greater than fingerprint ridges [7]. However, the effect of fingerprints on friction when in sliding contact with surface features much smaller than fingerprint ridge dimensions is a relatively unexplored territory. When studied at low normal loads typically used in tactile exploration of surfaces, studying the mechanisms of friction would help furthering the understanding of importance of friction in tactile exploration of surfaces. Understanding of the role of a finger's surface features on friction can help eliminate unimportant features during the design of skin-like surfaces for robotics and prosthetics applications.

In the present study, dry friction of micro-grit abrasive paper samples was measured for four different probing surfaces: human index finger pad, silicone finger replicas with and without fingerprints, and a smooth silicone sphere. The effect of countersurface and sliding orientation of finger and finger replicas on the coefficient of friction was examined. The role of finger prints, shape of the finger and the elastic properties of finger was investigated and possible friction mechanisms are proposed.

4.2 Materials and Methods

4.2.1 Materials

The three samples selected for friction testing were FEPA micro grit abrasive papers with grit sizes of P800, P1200 and P2500 and mean particle sizes of 21.8 µm, 15.3 µm and 8.4 µm respectively, per manufacturer standards. The corresponding roughness average (Ra) values measured using a contact profilometer (Mahr, MarSurf SD26) were 6.00 µm, 4.23 µm and 4.05 µm respectively. Scanning electron microscopy images of the abrasive papers confirmed that the sizes of the particles were in agreement with the particle sizes reported by the manufacturer.

Based on the relative sizes of their particles, the P800, P1200 and P2500 are henceforth referred to as coarse, medium and fine grits, respectively. The abrasive papers were cut into 65 x 20 mm strips and attached on to a 152 x 101 mm steel backing plate for testing purposes. Four different types of probe materials were used to test the friction properties: a human finger, a silicone replica of the human finger with finger prints, a silicone replica of the human finger without finger prints and a smooth silicone sphere, as shown in Figure 4.1. Silicone is one of the synthetic materials considered to be a reasonable mechanical equivalent to skin on fingers due to similar friction properties [4, 13] and the silicone samples were used in the current study to help isolate the effect of fingerprints and the probe (finger) shape on friction. All the tests with the finger were done by using the right hand index finger of one of the researchers. Both the silicone finger replicas with and without fingerprints were modeled after the same finger. Single-use alginate molds (Alja-Safe, Smooth-On Inc.) of the finger were used to cast silicone finger replicas with fingerprints using a platinum cure silicone rubber (Smooth-Sil 950, Smooth-On Inc.). The fingerprints on the human finger were masked and the masked finger was used to

make alginate molds for casting silicone finger replicas without fingerprints. The fingerprints were masked by applying thin coats of fingernail enamel layer by layer and with intermediate visual inspection to check the degree of masking. This process was used to obtain a finger replica with no fingerprints while retaining the large-scale dimensions and bulk shape of the finger. A dial caliper (Mitutoyo, 505-675) was used to check the consistency of dimensions between the human finger and silicone finger replicas. The cured mean durometer hardness of the silicone replicas was 50 Shore A. The silicone sphere (Ultra-strength Silicone Rubber Ball, McMaster-Carr) was 2.54 cm in diameter (the radius of curvature of the human finger for the contact zone in the current experiment is approximately 1.22 cm) and had durometer hardness of 51 Shore A. The mean durometer shore hardness of the human index finger pad was 33 Shore A. All hardness values were measured using an ASTM Type A durometer (PTC Instruments, Model 408).

Figure 4.1 Probing surfaces used: (a) Right hand index finger, (b) silicone finger replica with finger prints, (c) silicone finger replica without finger prints, and (d) silicone sphere. The inset images in 1(a) and 1(b) show the fingerprint details in the same area of the finger and the silicone finger replica with fingerprints.

4.2.2 Methods

The surface topography of the abrasive papers was examined using a scanning electron microscope. A FEI Quanta 250 Field emission SEM was used for iridium coated abrasive papers to obtain the images with three dimensional profiles of the abrasive paper surfaces. The SEM images were processed and analyzed using the image analysis software ImageJ.

For the friction property measurement, each of the probes was slid along the length of the abrasive-paper surfaces. The steel backing plates holding the abrasive papers were mounted onto the platform of a three-axis dynamometer (Kistler 9254), which was used to measure the normal load applied and the resultant tangential friction force during sliding. During the sliding motion, for the finger and the silicone finger replica samples, the sliding angle with respect to the surface was maintained between 30° and 45°. The sliding speed was maintained for all the probes between 0.8 cm/s and 1.2 cm/s. A normal load of 0.5 N with approximate variation of 0.05 N was applied manually using visual feedback from the dynamometer for all the probes tested. For a spherical surface in contact with a topographically rough flat surface, contact area is linearly proportional to the applied normal load[19]. During the pre-tests, it was noticed that the contact area of the finger and the silicone finger replicas changes with the sliding angle. In effect, the combination of the applied normal load and the sliding angle governs the contact area of the probe, and the alignment of the fingerprint ridges in the contacting area for the ridged probes (human finger and the silicone finger replica with fingerprints). At the applied normal load of 0.5 N, Figure 4.2 illustrates the effect of the sliding angle on the contact area of the human finger pad and the corresponding fingerprint ridge orientations. For the higher sliding angles (Figure 4.2(a) - 4.2(c)), all the fingerprint ridges were aligned more or less parallel to each other. For

lower sliding angles (Figure 4.2(d)), the fingerprint ridge alignment was more complex, and as such low angles were not employed in this study of fundamental friction mechanisms.

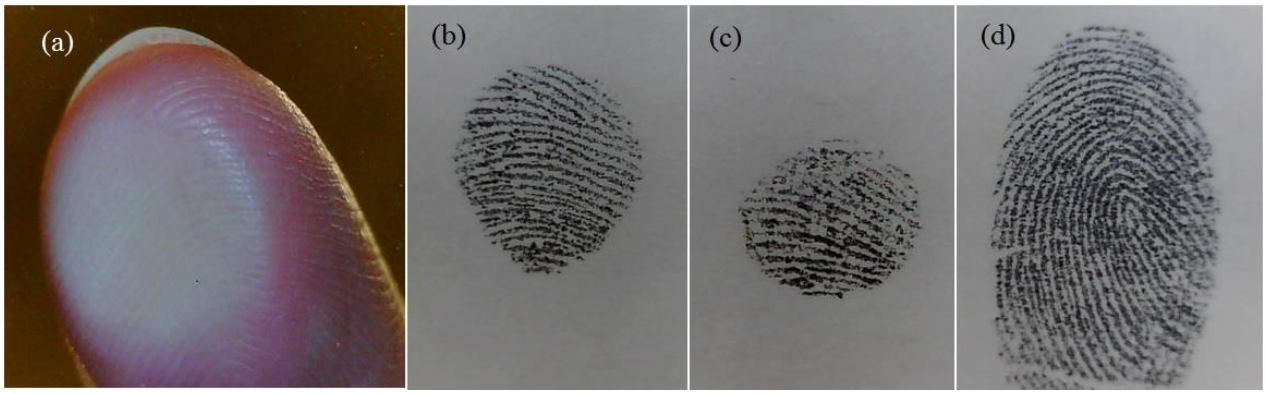

Figure 4.2 The contacting areas of different probing surfaces at normal load of 0.5 N. (a) Human finger pad at a sliding angle of approximately 37°. Impressions of human finger pad at sliding angles (b) ~37°, (c) ~85°, (d) ~10°. All the impressions are of same scale. All the images were obtained using a digital microscope (Dino-Lite Basic AM2111).

Based on a preliminary perception experiment done for a previous study, the results of which are presented elsewhere, it was observed by the participants and the researchers that sliding finger across abrasive papers felt different in different orientations of the finger with respect to sliding direction. In order to better understand the nature of this directionality, the friction properties were measured for two sliding orientations (shown in Figure 4.3): 1) a 'normal orientation', in which, the fingerprint ridges, for the normal load-sliding angle combination used in the current experiment, were normal / perpendicular to the direction of sliding. The length of the finger was in-line with the direction of the sliding; 2) a 'parallel orientation', in which, the fingerprint ridges were tangential / parallel to the direction of sliding. The length of the finger was perpendicular to the direction of sliding. For the silicone finger replica without fingerprints in spite of the lack of fingerprint ridges, the same orientation convention was used. For the silicone sphere, the surface is both symmetrical and smooth, and as a result, no orientation was assigned for sliding.

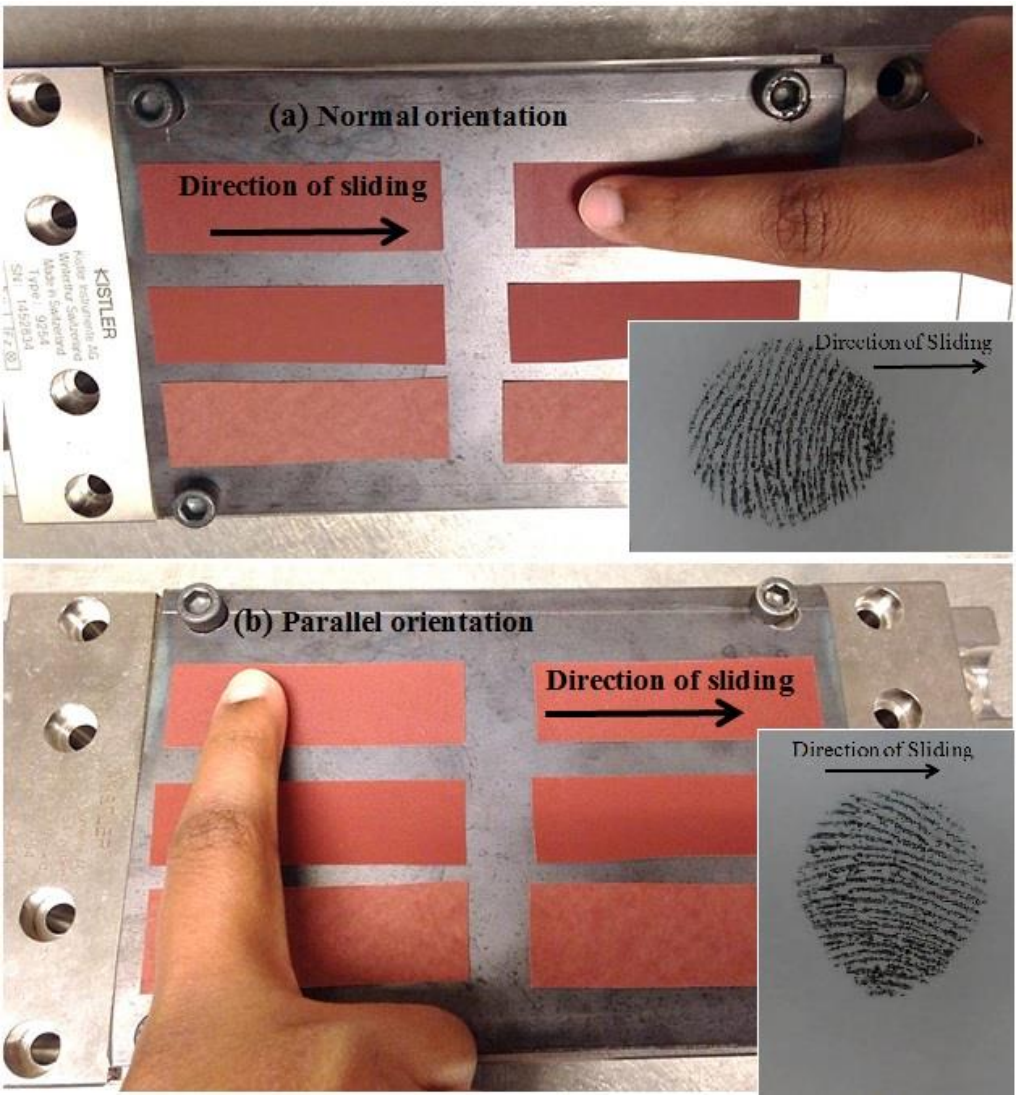

Figure 4.3 Sliding orientations used for the friction measurement tests. Finger sliding on P800 (coarse) grit abrasive paper mounted on a Kistler 9254 Dynamometer in (a) normal orientation, (b) parallel orientation. Inset images shows alignment of fingerprint ridges relative to the direction of sliding for the corresponding orientation. Orientations will be similar for the silicone replicas with and without fingerprints.

For the friction measurement, each trial constituted a single swipe across the length (sliding length of approximately 60 mm) of the abrasive paper sample with a probe. For each of the abrasive paper grits tested, when using a synthetic probing surface (silicone replicas with and without fingerprints and the silicone sphere), 6 trials were performed. Eleven trials were performed for tests with the human finger to account for higher variability. All friction measurements involving a single probe (66 trials for human finger and 36 trials each for rest of

the probes), were performed as a single set in a randomized order across abrasive papers and orientations. The random order changed from probe to probe. The normal loads used (0.5 ± .05 N) were typical of the loads used for tactile exploration [2, 20, 21]. The data acquisition system employed a LabVIEW program for data sampling at 1000 Hz. The coefficient of friction (COF) was calculated using Amonton's law at each time-step for the sampled data. A MATLAB program was employed to find the average coefficient of friction during a trial and, at least 1500 points were considered for computing the average for each trial. A wear particle build up on the surfaces of the probes and the abrasive papers was noticed during preliminary tests when more than 30 trials were performed at once. For finger friction measurements, the hands of the subject were washed and dried thoroughly every 11 measurements to minimize the effect of wear particles deposited during sliding, hydration of skin from sweat, and of oils secreted from the skin. For the silicone finger replicas, each replica was used only for 3 trials (a total of 12 replicas per measurements with each probe), to minimize the effect of the change in topographical features from surface wear and the wear particle build up. For the silicone sphere, the surface in contact was changed every three trials by rotating the sphere. All the friction measurements were performed in a temperature and humidity controlled laboratory setting with a temperature of 23 ± 2 ^{o}C and relative humidity of 50 ± 5 %.

4.3 Results and Discussion

4.3.1 Surface microstructure of abrasive papers

To better understand the friction behavior of the probing surfaces and identify the corresponding underlying friction mechanisms, it is imperative to have an understanding of the topography of the contacting asperities. The SEM images of the abrasive papers were used to

study their surface microstructure. The SEM images show that the sizes of the large dimension of the particles were in agreement with the particle size values provided by the manufacturer. The surface of the coarse and the medium abrasive papers consisted of sharp peaked pyramidal abrasive particles aligned mostly perpendicular to the surface of the backing paper with valley-like clear separation between the particles (Figures 4.4(a) and 4.4(b)). Whereas, the surface of the fine abrasive paper had thin plate like abrasive particles aligned more parallel than perpendicular to the surface of the backing paper and overlapping each other (Figure 4.4(c)).

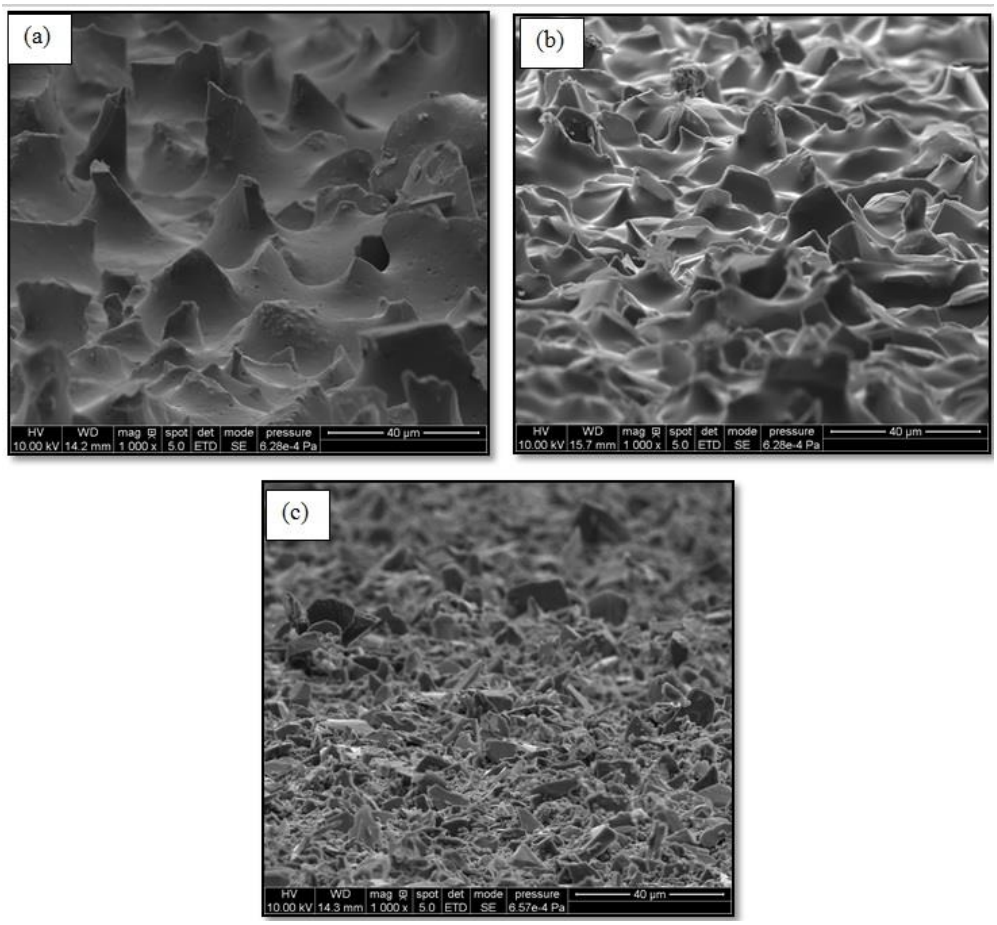

Figure 4.4 Scanning Electron Microscope images of abrasive papers (a) P800 (coarse) (b) P1200 (medium) (c) P2500 (fine). All images were secondary electron images at 1000X and 85° tilt. The horizontal scale bar is 40 µm in length.

4.3.2 Trends in the coefficient of friction

The coefficients of friction of the three abrasive papers, coarse, medium and fine, were measured against the four different probes in the two different sliding orientations (normal and parallel to the fingertip or simulant ridges). This was done to understand the effect of the shape, material properties and the presence of fingerprint ridges on friction during tactile exploration with texture elements smaller than the size of the ridges. The COF measurements from the sliding tests on abrasive papers with different probing surfaces were plotted as a function of the mean particle size of the abrasive papers to evaluate the trends in the coefficients of friction (Figures 4.5 and 4.7). The mean particle size was a defining variable that differentiates different abrasive paper grits, and was used for this reason as the independent variable for plotting COF values. The value of the mean particle size increased linearly from the fine to the coarse abrasive papers. Due to its symmetrical and featureless smooth surface, the friction properties of the silicone sphere did not have orientation effects, and the COF values for the silicone sphere were represented in plots for both the normal and parallel orientations.

The coefficient of friction of the silicone sphere decreased from the fine to the medium grits and then increased from the medium to the coarse grits. In the normal orientation of the human finger and the silicone finger probes with and without fingerprints, the same trend in COF values was observed. Also, in the parallel orientation of the silicone finger probe without fingerprints, the trend in COF from finest to the coarsest grit was the same. The amount of decrease from the fine to the medium and the amount of increase from the medium to the coarse grits was different for different probes. However, the decrease was dramatic for the human finger pad in the normal orientation. Also, for the human finger pad in the parallel orientation, the COF increased from the fine through coarse grits and, for the silicone finger with finger prints the

COF values increased from the fine to medium grits and then changed little (Figure 4.8). The possible reasons for such orientation dependent effects and the frictions mechanisms responsible are discussed in detail in the subsequent sections.

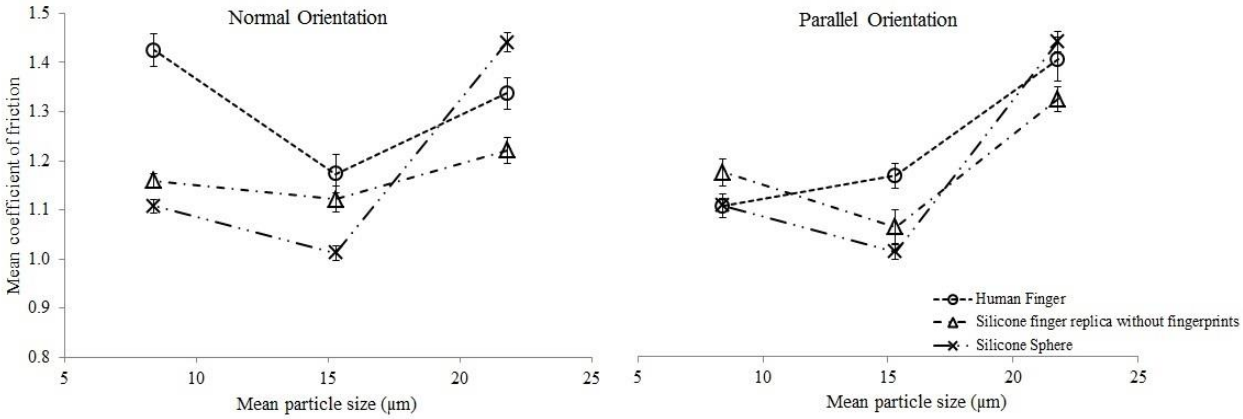

Figure 4.5 Variation of coefficient of friction of the abrasive papers for the human finger, the silicone finger replica without fingerprints and the silicone sphere as a function of the mean particle size of the abrasive papers in normal orientation and parallel orientations. Error bars indicate standard error of the mean coefficient of friction. The mean particle size of the fine, medium and the coarse grits are 8.4 μm, 15.3 μm and 21.8 μm respectively

4.3.3 Friction mechanisms

The net friction between the skin and a contacting surface has been suggested to be a summation of two terms: 1) adhesive friction and, 2) a deformation friction [22]. The adhesion friction results from breaking temporary bonds formed between the surface atoms of the interacting surfaces [23] and in the case of skin friction, adhesion coefficient of friction could be expressed by the equation:

$$\mu_a = \frac{\tau_0 A}{N} + \alpha \qquad (1)$$

where τ_0 is the interfacial shear strength, A is the real contact area between the interacting surfaces, N is the applied normal load and α is the pressure coefficient [22]. The equation suggests that the change in real contact area causes change in adhesion component of friction.

The deformation friction results from the imbalance of surface contact around an asperity due to the partial recovery (hysteresis) of the viscoelastic material, which is deformed by the rigid asperities of the interacting surface, and for a rigid conical slider interacting with an elastomeric surface, the deformation coefficient of friction due to hysteresis could be obtained from the equation derived by Greenwood and Tabor[24]:

$$\mu_h = \frac{2(1-\sigma^2)}{\pi E}\,\bar{p}\beta \tag{2}$$

where β is the hysteresis loss fraction, is the mean pressure defined as ratio of the normal and contact area, σ and E are the Poisson's ratio and elastic modulus respectively of the elastomer. It can be observed from this equation that the increase in the contact pressure or the decrease in elastic modulus could increase the deformation component of friction.

The repetitive motion of fingerpad on abrasive paper surfaces could result in scratching of the finger surface and abrasive wear. Deformation friction in such a scenario was termed as 'ploughing friction' by Derler et al. and the ploughing coefficient of friction obtained by modelling skin as an elastomeric surface in contact with a rigid conical sliders was given by the equation:

$$\mu_p = \frac{2}{\pi}\tan\phi \tag{3}$$

where ϕ is the mean slope of the conical sliders with the interface[15]. The ploughing friction clearly depends on the slope of the hard sliders with the softer interface and it can be said that shaper the indenter higher is the deformation component of friction.

In addition, a third interlocking term has been proposed to model the friction force for skin in contact with ridged surfaces. Interlocking friction arises from the resistance encountered

by the ridges of the finger climbing over the asperities of the interacting surface and was estimated the interlocking coefficient of friction for a triangular ridged surface in contact with finger pad as:

$$\mu_i = \cot \delta \tag{4}$$

where δ was the angle between triangular ridge and the vertical center line [7]. From the equation, it can be said that sharper the ridged surface greater is the interlocking component. The same could be applied for the abrasive particles sliding over the surface of the fingerpad. .

The silicone sphere had a nominally smooth featureless surface such that the friction properties were likely due to only adhesion and deformation mechanisms. The fine grit abrasive paper's surface topography consisted of flat closely aligned particles. This could lead to high real contact area when interacting with smooth surface like that of the silicone sphere, and consequently, a high adhesion component of friction. However, due to the same flat particle the deformation component of friction could be quite low. So, the net friction could be dominantly due to adhesion. For the medium and the coarse grits, with sharp peak-like particles, the adhesion between the abrasive papers and the silicone sphere could decrease due to decrease in the real contact area. However, the deformation friction could potentially increase due to the increase in the sharpness of the contacting asperities. The resultant coefficient of friction would be a combination of these two effects. The deformation component of friction could increase with the increase in size of the asperities. This could result in a higher deformation friction for the coarse grit compared to medium grit. From the COF data for the silicone sphere it was observed that, the COF for the fine grit was high, followed by a decrease in the COF leading to a minimum for the medium grit and then an increase with the increasing asperity size reaching a maximum for the coarse grit. Based on this COF trend, it would be safe to reason that adhesion was the

dominant mechanism for the fine grit, contributions from both adhesion and deformation components were reasonably important for the medium grit and deformation was the dominant mechanism for the coarse grit.

From the friction data it can also be observed that the COF for the silicone sphere for the coarse grit was the highest, and for the medium and the fine grits was the lowest compared to corresponding coefficients of frictions for the other probing surfaces and the same frictional trend could be seen in both the sliding orientations. This trend in COF for the silicone sphere combined with its symmetrical structure and a lack of identifiable surface features makes it ideal to be used as a baseline comparison for the other probes to understand the effects of their respective topography and material properties on the dominant friction mechanisms.

4.3.4 Effect of shape of the finger

Modifying the shape of the probe from silicone sphere to finger could change the contact area, whose positive changes lead to an increase in the adhesion component of friction and a decrease in the deformation component of friction. Depending on the dominating friction mechanism for a given interacting surface, the COF could change accordingly. The coefficients of friction of the silicone finger replica without fingerprints were compared with those of the silicone sphere to understand this effect (Figure 4.5).

The contact surface for the silicone sphere was a circle (Figure 4.6(a)), and that of the silicone finger replica was approximately an ellipse and (Figure 4.6(b)) with its minor axis similar to the radius of the circle. There was a measured increase in the contact area for silicone finger replica without fingerprints compared to the silicone sphere. The increase in the contact area could lead to an increase in the adhesion component of friction. The deformation component

of friction could decrease due to a decrease in the contact pressure. When compared with the silicone sphere, the net result would be an increase in the COF for the fine grit for which adhesion was the dominant mechanism and a decrease in the COF for the coarse grit for which deformation was the dominant mechanism. That was indeed the case with experimental COF values for the fine and coarse grits. For the medium grit, no meaningful prediction could be made without knowing the relative contributions of adhesion and deformation components to the friction. However, the experimental COF values suggest that adhesion friction could be contributing relatively more than the deformation component, as witnessed by the overall increase in the COF for the medium grit.

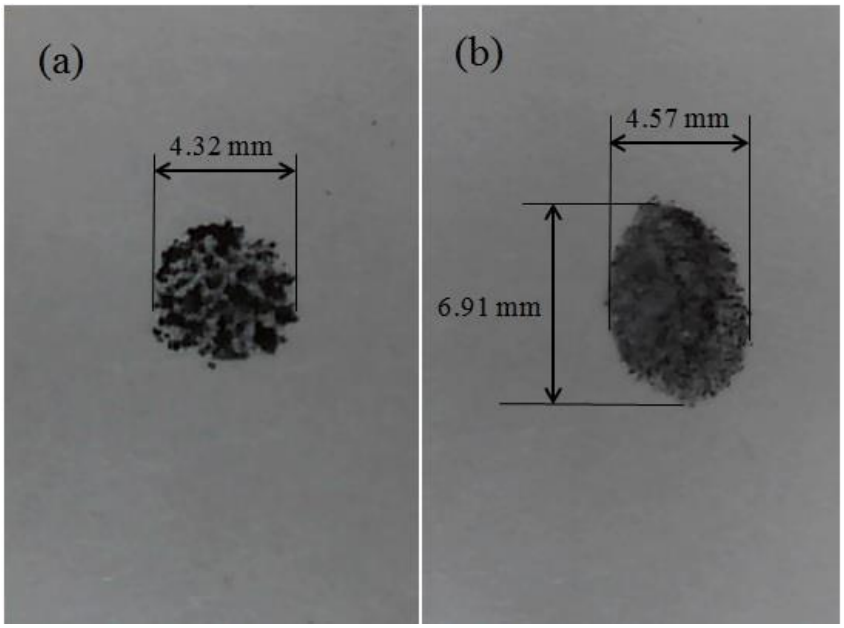

Figure 4.6 (a) Contacting area of the silicone sphere. (b) Contacting area of the silicone finger replica without fingerprints at a sliding angle of ~30°. All Impressions were scanned using a digital microscope (Dino-Lite Basic AM2111) and were measured using Image J image analysis software.

4.3.5 Effect of the fingerprints

The presence of fingerprint ridges could add an interlocking contribution to the coefficient of friction, and a possible decrease in the adhesion and deformation components.

However, the effect could be complex and vary with multiple factors like the shape and size of the contacting asperities, sliding direction of the finger and the angle of sliding. The effect of fingerprints was examined by comparing silicone finger replicas with and without fingerprints (Figure 4.7).

For the silicone replica with fingerprints, when compared with the silicone replica without fingerprints, the presence of fingerprint grooves could decrease the real contact area, decreasing the adhesion component of the coefficient of friction. Also, the presence of grooves could decrease the penetration of asperity into the silicone finger surface in the groove space, resulting in a decrease in the deformation component of friction. Decrease in both of these components depends on the width of the fingerprint groove. Further, for the silicone replicas with fingerprints, interlocking could take place when the asperities of the abrasive papers pass from inside the grooves of the fingerprints over to the top of the ridges of the fingerprints. The contribution of interlocking depends on the relative sizes of depth of the fingerprint groove and the height of the asperities. The alignment of the fingerprint ridges in the contacting area combined with the sliding direction determines the zone in which interlocking can happen. At the sliding angles and the normal load employed in the current study, the fingerprint ridges in the contacting area were all aligned and oriented in the same direction, and the interlocking effect was possible only in the normal orientation.

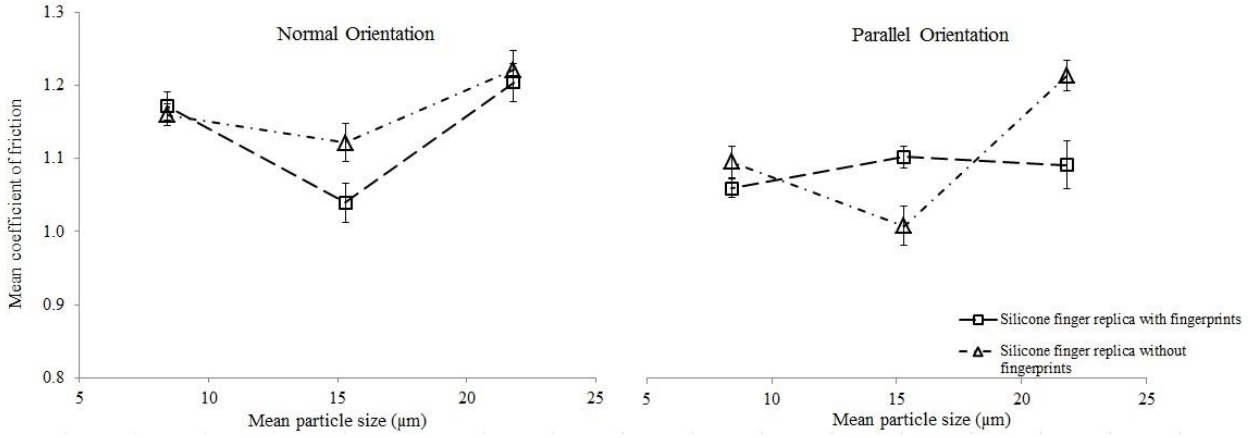

Figure 4.7 Variation of coefficient of friction of the abrasive papers for the silicone finger replicas with and without fingerprints as a function of the mean particle size of the abrasive papers in normal and parallel orientations. Error bars indicate standard error of the mean coefficient of friction.

In the normal orientation of the silicone replicas with fingerprints, the fingerprint ridges were perpendicular to the direction of motion of the finger (Figure 4.3(a)) and the interlocking was possible during relative motion of fingerprint ridges over the surface asperities of the abrasive papers. The effects of interlocking however depend on the relative sizes of contacting asperities[7]. For the human finger, the ridge width and groove widths are approximately 400μm and 150μm respectively [9] and the depth of the groove was approximately 25μm [17]. For the fine grit, with very small flat particles (mean particle size 8.4μm) aligned almost parallel to its surface, the increase in COF from interlocking would be small and there could be a slight decrease in the adhesion component of friction due to decrease in real contact area in the groove space. The COF would be more or less the same for the replicas with fingerprints and the replicas without fingerprints. This was in agreement with the experimental values of COF. For the medium grit (mean particle size 15.3μm), interlocking could take place. The deformation component of friction could decrease due to a decreased penetration of asperities in the groove space and the adhesion component of friction due to loss of contact in the groove space. The COF however would depend on the relative contribution of interlocking compared to the other two components. The decrease in the experimental coefficient of friction value of the silicone

replicas with fingerprints from that the silicone replicas without fingerprints suggests that the asperities were still small enough for any considerable interlocking effects to take place. For the coarse grit (mean particle size 21.8μm), the size of asperity might be close enough to the depth of the fingerprint grooves to create significant interlocking effects. However, the deformation component of friction could decrease due to lack of deformation in the groove space. The net effect would depend on the whether contribution of interlocking was sufficient to offset the decrease in deformation component. There was no change in the experimental value of COF from silicone replicas without fingerprints to the replicas with fingerprints, suggesting that interlocking was indeed possible.

For the parallel orientation, the fingerprint ridges were parallel to the direction of motion of the finger (Figure 4.1(b)) and the effect of fingerprints was a slight decrease in COF for the fine grit, an increase for the medium grit and a dramatic decrease for the coarse grit. Very little interlocking effect was assumed to be possible as the relative motion of the asperities of the abrasive papers was either along the edge of the ridge, in the grove or on top of the ridge. Based on the fingerprint ridge and groove dimensions, the size of the abrasive paper asperities and spacing between abrasive paper asperities, the following are possible explanations from the trends in the coefficient of friction. For the fine grit, considering the relative sizes of asperities and the depth of the fingerprint groove, the asperities that lie in the fingerprint groove could have no contact with the groove surface. The additional contact area from the asperity contact along the edge of the ridge was negligible due to flat plate like nature of the fine grit's abrasive articles (Figure 4.4(c)). This could result in a decrease in the adhesion friction due to the decrease in the real contact area and in turn the decrease in the COF. For the medium grit, the adhesion component of the friction could increase from the increase in the number of asperity surfaces in

contact along the edges of the ridges. From the asperities moving in the grooves, there could be no possible contribution to the deformation of the probe surface and could result in a decreased deformation component of the friction. The net effect however would depend on relative contributions of adhesion and deformation components to the friction. The increase in the experimental COF supports that previous observation about the adhesion friction possibly contributing relatively more than the deformation component for the medium grit. For the coarse grit, due to its larger asperities, the loss of deformation could be higher from the asperities moving in the grove. With the deformation hypothesized to be the dominant contributor to the friction, the effect of decrease in deformation friction could be more dramatic on the net friction in comparison with the effect of increase in adhesion friction. The decrease in the coefficient of friction from silicone replicas without fingerprints to that of the replicas with fingerprints for the coarse grit supports the hypothesis.

4.3.6 Effect of the material properties in combination with the fingerprints

The effect of material properties in combination with the fingerprints was analyzed by comparing the human finger pad friction values with those of the silicone replica with fingerprints (Figure 4.8). The effect of change in material properties from silicone replica to a finger was a marked increase in all the three components of friction. However, there were some possible interaction effects between the interlocking and adhesion mechanisms, as well as between the interlocking and deformation mechanisms.

Elastic modulus of the probing surfaces can be roughly estimated using their durometer shore hardness values using Gent's semi empirical relation[25]. The durometer shore hardness of the human finger pad (32 Shore A) was less than that of the silicone replicas with fingerprints

(50 Shore A) and from Gent's relation, the elastic modulus of the finger was less than that of the silicone samples. The lower elastic modulus could enable the surface of the skin to conform itself around the countersurface asperities more than the silicone. This could increase the adhesion component of friction due to increased real contact area and the interlocking component of the friction whenever interlocking was possible. That is, wherever interlocking was possible, for a given normal load, finger-on-asperities had higher probability of interlocking to take place than the silicone replica with fingerprints. Also, when interacting with countersurface asperities of given hardness (greater than that of human skin or silicone allowing their deformation), localized deformation for finger pad could more due to its lower shore hardness than that of the silicone replica. This could increase the deformation component of friction.

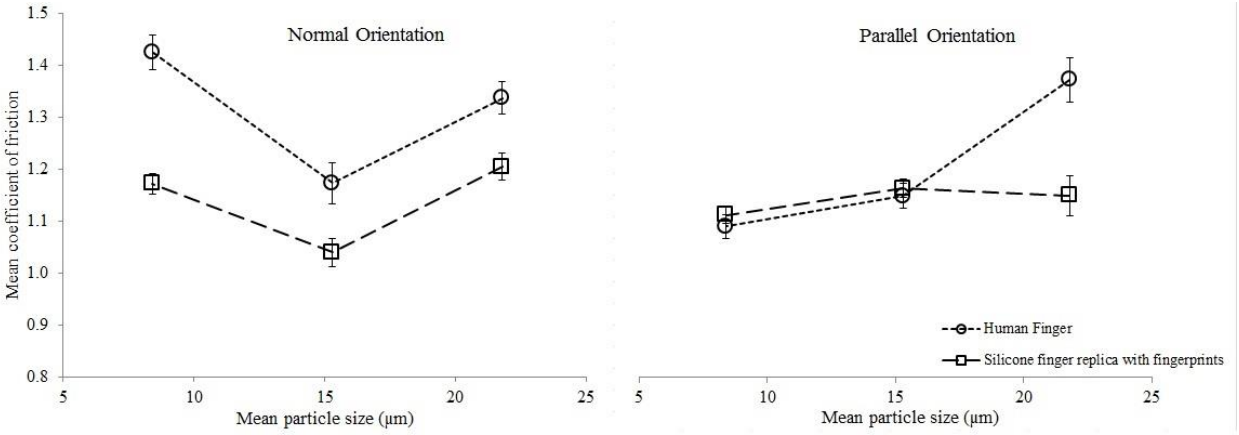

Figure 4.8 Variation of coefficient of friction of the abrasive papers for the human finger and the silicone finger replica with fingerprints as a function of the mean particle size of the abrasive papers in normal and parallel orientations. Error bars indicate standard error of the mean coefficient of friction.

For the normal orientation, there was a possibility of interlocking to happen for both the human finger and the silicone replica. For all the three abrasive paper grits, there was an increase in the mean coefficients of friction of human finger compared to those of the silicone replica with fingerprints. Based on the hypothesized dominant friction mechanisms for each of the grits, for the fine grit, the increase could be due to a combination of the increase in adhesion and

interlocking components of friction. It is believed that for the medium grit, the increase could from an increase in the interlocking component and for the coarse grit, the increase could be from a combination of the interlocking and deformation friction components. However, for the coarse grit the increase in the coefficient of friction in the normal orientation was less marked than that in the parallel orientation. It was possible for the interlocking action to create harder zone ahead of it leading to a decrease in the amount of deformation and a consequent decrease in the deformation component of the friction.

For the parallel orientation, no interlocking effect was possible for either of the probes. There was little change in the coefficients of friction of the fine and the medium grits for human finger when compared to those for the silicone replica with fingerprints. This suggests that interlocking component could indeed have been responsible for increase in the coefficients of friction for the fine and the medium grits. However, the possible increase in adhesion friction component for the fine grit was more pronounced in the normal orientation and was not as evident in the parallel direction. One probable explanation was bending of fingerprint ridges in the direction of motion of the finger as the as the asperities of the abrasive paper move over them in the normal orientation. The bending could have caused an increased contact area and a consequent increase in the adhesion friction. Due to the lower elastic modulus of the finger, this effect would likely be more pronounced than for the silicone replica. For the coarse grit, the increase in COF could be from an increase in the deformation friction.

4.4 Conclusions

In this study, coefficients of friction of micro-grit abrasive papers for index finger pad and different silicone surfaces were measured at normal loads typically used for tactile

exploration. The goal was to isolate the effects of fingerprints, shape and material properties of the finger and the finger replicant probes. Possible friction mechanisms involved were discussed. The following conclusions can be drawn from the results of this study.

- The fingertip coefficient of friction when interacting with textured surfaces of small elements (<50 μm) showed strong evidence of obeying a summation of adhesion, deformation and interlocking components.
- The shape of the finger was responsible for an increase in contacting surface area, which further affected the adhesion and deformation components of friction. Thus, probe shape appeared to have a significant impact on the overall coefficient of friction.
- The presence of fingerprint ridges is hypothesized to add an interlocking contribution to the overall coefficient of friction, based on the results. The contribution of interlocking friction can vary with multiple factors like the shape and size of the contacting asperities, sliding direction of the finger and the angle of sliding. Further, the fingerprint ridges appeared to cause a decrease in the deformation and the adhesion components of friction.

4.5 References

[1] Westling, G., Johansson, R. Factors influencing the force control during precision grip. Exp Brain Res 53:277-284 (1984).

[2] Smith, A., Gosselin, G., Houde, B. Deployment of fingertip forces in tactile exploration. Exp Brain Res 147:209-218 (2002).

[3] Lewis, R., Menardi, C., Yoxall, A., Langley, J. Finger friction: Grip and opening packaging. Wear 263:1124-1132 (2007).

[4] Derler, S., Schrade, U., Gerhardt, L.C. Tribology of human skin and mechanical skin equivalents in contact with textiles. Wear 263:1112-1116 (2007).

[5] Darden, M.A., Schwartz, C.J. Investigation of skin tribology and its effects on the tactile attributes of polymer fabrics. Wear 267:1289-1294 (2009).

[6] Tomlinson, S.E., Lewis, R., Carré, M.J. The effect of normal force and roughness on friction in human finger contact. Wear 267:1311-1318 (2009).

[7] Tomlinson, S.E., Carré, M.J., Lewis, R., Franklin, S.E. Human finger contact with small, triangular ridged surfaces. Wear 271:2346-2353 (2011).

[8] Tomlinson, S., Lewis, R., Liu, X., Texier, C., Carré, M. Understanding the Friction Mechanisms Between the Human Finger and Flat Contacting Surfaces in Moist Conditions. Tribol Lett 41:283-294 (2011).

[9] Derler, S., Gerhardt, L.C., Lenz, A., Bertaux, E., Hadad, M. Friction of human skin against smooth and rough glass as a function of the contact pressure. Tribology International 42:1565-1574 (2009).

[10] Pasumarty, S., Johnson, S., Watson, S., Adams, M. Friction of the Human Finger Pad: Influence of Moisture, Occlusion and Velocity. Tribol Lett 44:117-137 (2011).

[11] Tomlinson, S.E., Lewis, R., Carré, M.J., Franklin, S.E. Human finger friction in contacts with ridged surfaces. Wear 301:330-337 (2013).

[12] Shao, F., Childs, T.H.C., Henson, B. Developing an artificial fingertip with human friction properties. Tribology International 42:1575-1581 (2009).

[13] Hyun-Yong, H., Shimada, A., Kawamura, S.: Analysis of friction on human fingers and design of artificial fingers. pp. 3061-3066. Place (1996)

[14] Masen, M.A. A systems based experimental approach to tactile friction. Journal of the mechanical behavior of biomedical materials 4:1620-1626 (2011).

[15] Derler, S., Preiswerk, M., Rotaru, G.M., Kaiser, J.P., Rossi, R.M. Friction mechanisms and abrasion of the human finger pad in contact with rough surfaces. Tribology International 89:119-127 (2015).

[16] Prevost, A., Scheibert, J., Debrégeas, G. Effect of fingerprints orientation on skin vibrations during tactile exploration of textured surfaces. Communicative & integrative biology 2:422 (2009).

[17] Scheibert, J., Leurent, S., Prevost, A., Debrégeas, G. The role of fingerprints in the coding of tactile information probed with a biomimetic sensor. Science (New York, NY) 323:1503 (2009).

[18] Wandersman, E., Candelier, R., Debrégeas, G., Prevost, A. Texture- induced modulations of friction force: the fingerprint effect. Physical review letters 107:164301 (2011).

[19] Adams, M.J., Johnson, S.A., Lefèvre, P., Lévesque, V., Hayward, V., André, T., et al. Finger pad friction and its role in grip and touch. Journal of The Royal Society Interface 10:20120467 (2013).

[20] Smith, A.M., Scott, S.H. Subjective scaling of smooth surface friction. Journal of neurophysiology 75:1957 (1996).

[21] Smith, A., Chapman, C., Deslandes, M., Langlais, J.-S., Thibodeau, M.-P. Role of friction and tangential force variation in the subjective scaling of tactile roughness. Exp Brain Res 144:211-223 (2002).

[22] Adams, M., Briscoe, B., Johnson, S. Friction and lubrication of human skin. Tribol Lett 26:239-253 (2007).

[23] Stachowiak, G.W.: Engineering Tribology. Butterworth-Heinemann, (2006)

[24] Greenwood, J.A., Tabor, D. The Friction of Hard Sliders on Lubricated Rubber: The Importance of Deformation Losses. Rubber Chemistry and Technology 33:129-141 (1960).

[25] Gent, A.N. On the Relation between Indentation Hardness and Young's Modulus. Rubber Chemistry and Technology 31:896-906 (1958).

CHAPTER 5. INVESTIGATION OF THE ROLE OF FRICTION AND SAMPLE AREA ON THE TACTILE DISCRIMINATION OF TEXTURES

G.P. Chimata and C.J. Schwartz

Abstract

Tactile discriminability of non-patterned textured surfaces was studied to determine the effect of change in texture sample area on the differentiability of those textures. A perception measurement experiment in combination with a friction measurement experiment was performed to understand the possible role of friction in touch-based texture discrimination. Circular samples of the P800, P1200 and P2500 grit abrasive papers of three different sizes, 38.1 mm, 9.5 mm and 3.2 mm, referred to as large, medium and small sizes were used as stimuli. Same size samples were presented in pairwise combinations to determine the mean probabilities of differentiation for a texture pair at different sizes. Results from the perception measurement indicated that decreasing size of the texture sample resulted in a decrease in the ability to both reliably differentiate different-grit pairs and reliably identify same-grit pairs. Finger friction measurements from the participants suggested a possible edge effect on the friction of the samples. Friction measurements of the abrasive paper samples sliding against two silicone probes and scanning electron microscopy of the edges of the texture samples were also conducted to investigate the possible involvement of friction with tactile differentiation.

5.1 Introduction

Tactile discrimination of textures involves differentiating surfaces by processing information received through touch, likely involving complex interactions with surface parameters such as roughness, hardness, slipperiness and warmth of the surface. Human sense of touch has been shown to be superior to vision for discriminating textured surfaces, especially of finer textures[1]. Tactile discrimination tasks Early studies involving discrimination tasks focused on finding height detection thresholds and corresponding neural events for a single raised dot, and noticed that the detection thresholds decreased with an increase in the dot diameter[2, 3]. In a discrimination task involving two dot patterned surfaces, the difference in the spatial period of the surfaces was proportional to the discriminative performance[4]. In a discrimination study involving gratings of different roughness scales, the spatial period was found to be the most relevant dimension for texture discrimination[5] . These studies were quite informative in identifying the dimensions that were important during a discrimination event, but they were limited to only two types of textures (gratings and dot patterns) and rough textures at that. Discrimination tasks were also used to compare the texture perception ability of blind and sighted observers[1, 6]. Miyaoka et al. measured the discrimination thresholds for fine textured surfaces (sandpapers and gratings as stimuli) and proposed that the amplitude information of the roughness profiles was used for tactile discrimination [7]. A more recent study showed that wrinkled surfaces with amplitude as low as 13 nm could be successfully discriminated from blank surfaces, and proposed that the perceptual dimensions involved could be related to the coefficient of friction and the wavelength of the wrinkles[8]. The literature strongly suggests that topological information about the surface of the texture dictates differentiability of the textures.

However, the role of the size/dimensions of the texture sample size on the ability to discriminate between different textures is not clear and has not been thoroughly explored.

In this study, the authors aimed to determine the effect of sample area of non-patterned textures on the tactile differentiability of those textures and investigate the possible role of friction on the ability to discriminate among textures. With this objective, a perception measurement experiment was conducted in combination with participant's finger friction measurement. Friction measurements were also made for two silicone probes sliding against the stimuli used in the perception and finger friction measurement experiments. Results from all four experiments in combination with Scanning electron microscope images of the abrasive paper samples were analyzed.

5.2 Experimental Methods

5.2.1 Stimuli

Three FEPA fine grit abrasive papers P800, P1200 and P2500 (1913 siawat FC, Sia Abrasives Inc.) were used as the stimuli. In a previous study, these three grit abrasive papers, when provided in 78 x 90 mm sheets to the participants in a sequential manner, were clearly differentiated from each other (mean probabilities of detecting a difference were 0.93, 0.93 and 0.71 for P800-P1200, P800-P2500 and P1200-P2500 pairs respectively)[9]. The surface properties of the abrasive papers were listed in Table 5.1[9].

Table 5.1 Surface Properties of abrasive papers

Grit	Average Roughness Ra(μm) ± SE	Root mean square roughness Rrms(μm) ± SE	Mean spacing of profile peaks Rs(μm) ± SE
P800	6.00 ± 0.18	7.72 ± 0.20	105.68 ± 1.96

Table 5.1 continued.

P1000	5.69 ± 0.15	7.16 ± 0.18	74.52 ± 2.44
P1200	4.22 ± 0.10	5.31 ± 0.13	73.52 ± 1.53
P1500	3.98 ± 0.085	5.11 ± 0.13	64.10 ± 2.98
P2000	3.64 ± 0.034	4.59 ± 0.059	64.38 ± 2.40
P2500	4.05 ± 0.062	5.05 ± 0.093	62.77 ± 2.65

All surface roughness parameters of the abrasive papers were measured using a contact profilometer (Mahr, MarSurf SD26), and the standard errors were calculated for 5 trials for each of the parameters. The sliding direction of the stylus tip was parallel to the grit number printing on the back of the abrasive papers for all the trials considered.

Scanning Electron Microscopy (SEM) (FEI Quanta 250 Field SEM) was used to verify that the maximum particle dimensions of the abrasive papers were in agreement with the FEPA standard grain sizes (21.8 µm, 15.3 µm and 8.4 µm respectively for the P800, P1200 and P2500 grits). Circular samples of each of the three abrasive paper grits of three different diameters, 38.1 mm, 9.5 mm and 3.2 mm, respectively, were used for both the perception and friction experiments. The three sample diameters will hence forth be referred to as ‘large’, ‘medium’ and ‘small’ sizes respectively. Figure 5.1 shows the large, medium and small samples of P800 grit.

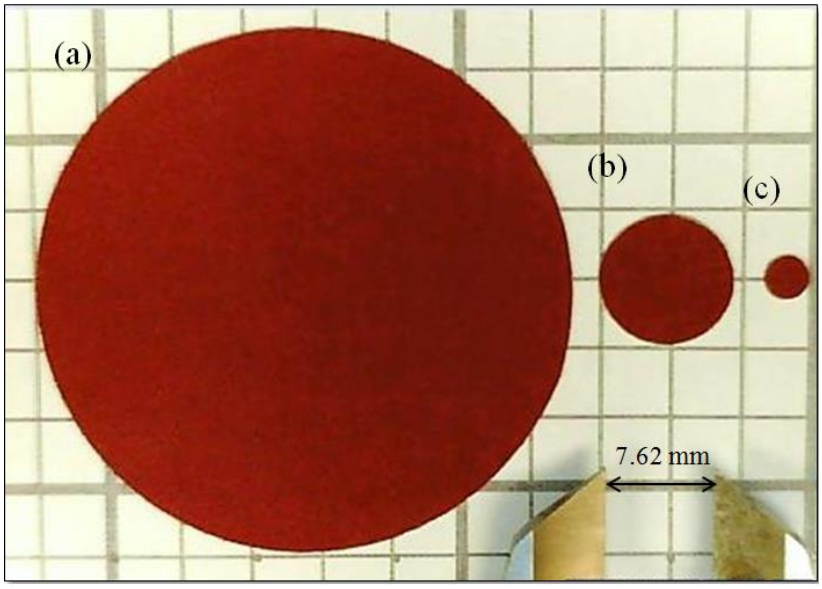

Figure 5.1 Circular samples of the abrasive paper grit P800 of the sizes (a) Large, (b) Medium and (c) Small. Scale bar was shown to give an estimate of the relative sizes of the samples.

In order to prepare the texture samples of different sizes, one of the adhesive sides of double sided adhesive sheets (Silhouette, 8.5-inch by 11-inch) was attached to the back of the abrasive papers and circle punches (EK tool punches, Simplicity.com) with diameters corresponding to the large, medium and small sizes were used to punch out the circular samples. This process enabled producing circular samples with consistent size and layer thicknesses (of abrasive and adhesive layers) across all sample sizes for all the abrasive grits. The sample diameters were verified by using a digital microscope (Dino-Lite Basic AM2111) and found to be within ± 0.1 mm. The texture samples were attached to smooth printer paper which in-turn was attached to a rectangular magnetic film by using a double sided tape. Textures of the same size were presented to the participants in pairwise combinations for the perception and friction measurements. For each size, there were 6 pairwise combinations of the abrasive papers (3 same pair and 3 different pair combinations). Each combination in-turn was repeated 4 times in an order randomized over the size and pairs tested, resulting in a total of 72 measurements (3 sizes x 6 combination x 4 repetitions) per each task (perception/friction) for each of the participants. The sample pairs were attached to the substrate with a constant gap size of 40 mm between the samples for all the three sizes. The texture samples mounted on the magnetic substrate constituted a sample configuration. The magnetic backings were of three different sizes (large, medium and small) corresponding to the three different sized texture samples as shown in Figure 5.2. The sizes of the magnetic backing were specifically designed this way to accommodate for the size of the textures as well as help guide the participants' finger to move in a straight line over the textures, especially for the medium and small sizes.

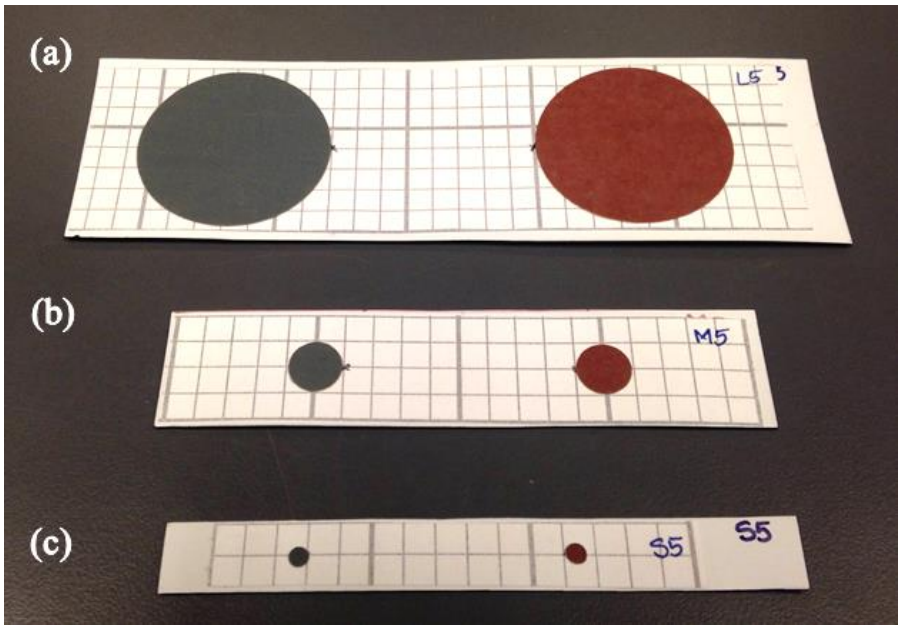

Figure 5.2 (a) Large, (b) Medium and (c) Small sample configurations for the abrasive grit pair P1200-P2500 corresponding to the large, medium and small texture samples. Different sized printing paper and magnetic sheets used for each can be seen.

5.2.2 Test subjects

A total of 23 subjects, 12 male and 11 female participated in the perception and human friction measurement experiment. The participants were recruited through convenience sampling, i.e. from the personal and professional contacts of the researchers, and from participant responses to the electronic and paper advertisements, as well as through snowball sampling. All the recruitment methods were approved by the institutional review board. All participants were above the age of 18, and all were right-handed. The recruited volunteers participated in a perception measurement task immediately followed by a friction measurement task. The participation in the study involved two 60-minute sessions per participant and the participants were allowed to schedule each of the study sessions either on the same day or different days according to their convenience. The full study was conducted over a period of 2 months. At the beginning of each session, the experimental procedures were explained to the participants, informed consent was obtained, and participants were given an option to stop the

experiment at any point. All participants completed both the sessions. To minimize the effect of the oils, sweat and wear debris from the skin, participants were instructed to clean their hands using alcohol wipes (CVS Isopropyl Rubbing Alcohol 70% Wipes) before the beginning of the perception and friction experiments and also periodically throughout the course of the experiments. All testing was conducted in a temperature controlled laboratory setting at a room temperature of 22 °C.

5.2.3 Perception measurement

The set up for the perception experiment was similar to the one used in 'Tactile discrimination sensitivity measurement' in Chapter 3 Section 3.2.1.3. During the perception measurement task, participants were seated across the table from the researcher. An opaque screen with curtained opening enabled the participants to access the test stimuli without providing any visual cues about the nature of the stimuli. The perception measurement involved a discrimination task and employed a two-alternative forced choice technique, with the two stimuli being presented with a fixed physical gap. This is in contrast to the previous study, where the pairs of textures for comparison were given to the evaluators sequentially in time, one after the other. For each comparison, the magnetic backing sheet with the test stimuli pair was placed on a thin steel support plate (150 mm X 50 mm X 0.7938 mm) and was presented to the participant. The participants were asked to hold one corner of the steel support plate with the non-dominant hand and swipe the index finger of the dominant hand from left to right at a steady pace along the length of the paper surface to assess the circular textures. After a maximum of two swipes, participants were asked to inform the researcher if the two textures were determined to be the same or different. The participants were instructed to use any sliding angle as per their

comfort except 0° or 90 °. However, they were instructed to keep the sliding angle and the sliding speed as consistent as possible for all the comparisons. The sliding angle was visually observed by the researcher to be between 30°-45° approximately for all the participants. Oval raised guiding dots were placed on the center of the left and right edges of the steel support sheet to help the participants move their finger in a straight line passing through the centers of the circular textured (abrasive paper) samples. Figure 5.3 shows the arrangement which was used to present textures to the participants. The same steel support plate was used for all 72 comparisons with appropriate magnetic sheet changed for each comparison. Further, each magnetic sheet with a sample pair was discarded after every two repetitions to minimize the effect of wear of samples on perception. That is, a total of 36 magnetic sheets (12 large, 12 medium and 12 small) were used per participant for the perception task.

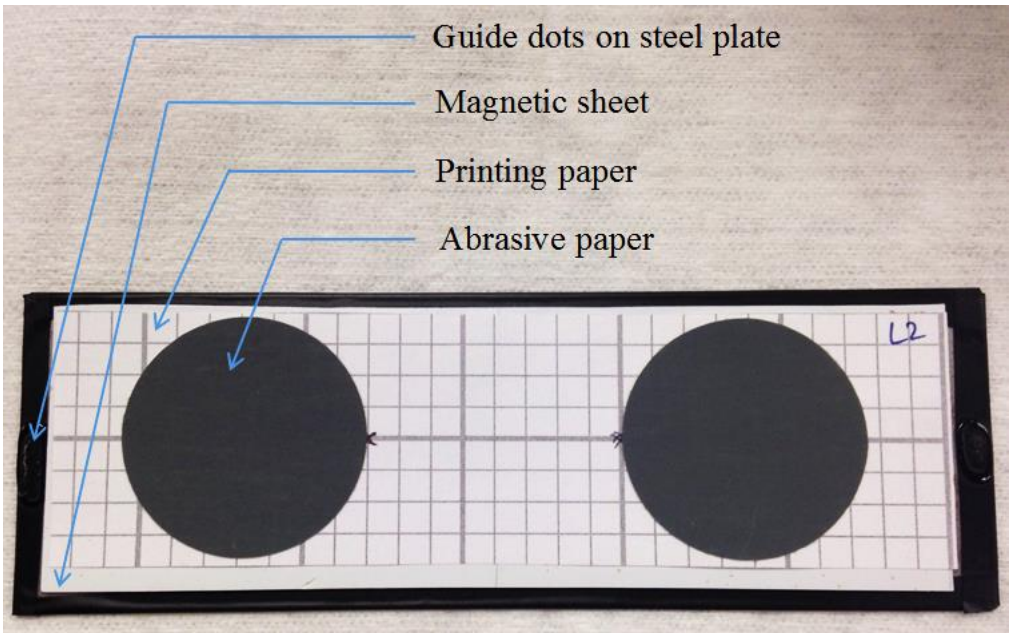

Figure 5.3 Large size P1200 – P1200 abrasive grit pair sample configuration. Steel support plate with raised guide dots at the ends was used to hold the magnetic sheet.

5.2.4 Human finger friction measurement

The same stimuli configurations used in the perception measurement test were used for the friction measurement test. A steel support plate (152.4 mm X 101.6 mm X 4.8 mm) was attached to a three-axis force transducer (Kistler 9254), and for each measurement, magnetic sheet with the appropriate sample pairs was placed on the steel plate. The participants were asked to use sliding motion of the index finger pad of the dominant hand from left to right at a steady pace similar to the one used in the perception task, and at a similar sliding angle with two consecutive swipes. The normal and friction forces during the swipe were recorded using a LabVIEW data acquisition program at a data sampling rate of 1000 Hz. Similar to the perception measurement experiment, each magnetic sheet with a sample pair was discarded after two repetitions.

5.2.5 Synthetic probe friction measurement

Two different synthetic probes, a smooth silicone sphere and a silicone finger replica were used to evaluate effect of the size of the stimuli on the friction behavior. A multi-axis tribometer (Rtec Instruments) was used to conduct the friction measurements with both the silicone probes. A 150 mm X 150 mm X 6.4 mm steel plate was attached to the motion controlled platform of the tribometer which allowed for the X-direction (left to right) and Y-direction (front to back) motion of the steel plate. The magnetic sheets with the appropriate sample configuration were placed on the steel plate for each measurement. A two-axis 10 N load cell capable of measuring friction and normal forces, respectively, of 10 ± 0.001 N was attached to the friction arm of the tribometer. A 6.4mm-diameter coated aluminum shaft with a threaded end attached to the load cell was used to hold the silicone probes. At the beginning of each

measurement, the silicone probe was brought in contact with the surface of the printing paper until the sensor read an initial normal force of 1.5 N and then the test was run with the 'Z' (normal) position of the probe held constant throughout the measurement. During the pre-tests with both the probes, researcher's attempts to conduct a normal load control test revealed the sensor's inability to handle the surface height change from backing paper to the texture resulting in normal load as well as Z-position fluctuations during the measurement. This prompted the researchers to use the position controlled test method described above. The swipe began with counterface motion from right to left. Sliding speed was constant for all measurements and was set at 10 mm/s. The friction and normal loads were recorded during the swipe using a custom program and the data was sampled at the rate of 1000 points per second.

5.2.5.1 Silicone sphere

The silicone sphere (8945K55, McMaster-Carr) was 25.4 mm in diameter and had durometer hardness of 51 Shore A. The stimuli configuration for the friction measurements with the silicone sphere was same as the one used in the perception and the human friction measurements (two circular texture samples in pairwise combinations with a fixed distance of 40mm between them). The sliding length was 130mm, 100 mm and 80 mm respectively for the large, medium and small sample configurations. For the silicone sphere, 72 friction measurements corresponding to 4 repetitions each of 6 pairwise combinations of the three textures with three stimuli sizes were obtained in a randomized order. The silicone sphere was rotated every 12 measurements such that a new surface is in contact to minimize the effect of wear of the sphere's surface on the friction measurements. 3mm radial holes were drilled into the

silicone sphere allowing the threaded end of the aluminum shaft to snugly connect. The holes were drilled at different locations on the surface of the sphere to accommodate for the rotation.

5.2.5.2 Silicone finger replica

The silicone finger replica was modeled after the right-hand index finger of one of the investigators. The negative of the finger was captured in an alginate mold (Alja-Safe, Smooth-On Inc.) and was used to cast a silicone finger replica with a tin-cure silicone rubber (Soft 107 Shore A, MPK Enterprises). The cured silicone finger had a durometer hardness of 5 Shore A. Pre-tests with the silicone finger replica showed that, as the finger replica slid along the length of the sample surface there was a decrease in the normal load due to the bending of the finger opposite to the direction of the sliding. However, this decrease in the normal load due to bending stabilized at a distance of approximately 40mm from the starting point of sliding. The sample configurations were designed to accommodate for this bending effect and only one texture sample was affixed to the printing paper. The circular samples were attached such that the stimulus' surface began at 75mm from the edge of the paper. The sliding length was 125mm, 105 mm and 95mm respectively for the large, medium and small sample configurations. For the silicone finger, 72 friction measurements corresponding to 8 repetitions each of the 3 textures with three stimuli sizes were obtained. To minimize the effect of the wear of the finger replica on friction, a new silicone finger replica was replaced after every 12 measurements and a total of 6 replicas were for the entire test. The silicone finger replicas were cast with a 5.8mm cylindrical hole through them and a 63 mm long bent aluminum shaft with bending angle of 120° was used to connect the silicone finger to the coated aluminum shaft. This arrangement helped slide

silicone finger replicas at a sliding angle of 30°. Figure 5.4 shows the silicone sphere and silicone finger probes with their corresponding stimuli configurations.

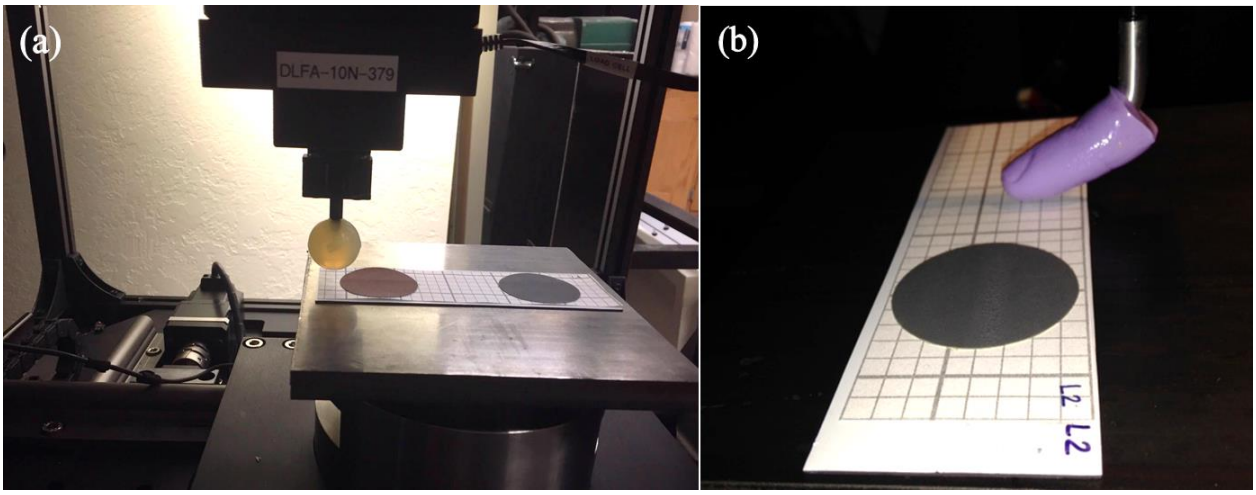

Figure 5.4 Silicone probes attached to the 10N load cell of the Rtec Tribometer with the samples attached to movable platform. (a) Silicone sphere and it's corresponding sample configuration two circular textures (P800-P1200 grit pair), (b) Silicone finger replica fixed at a sliding angle of 30° and the corresponding sample configuration with once circular texture (P1200 grit).

5.3 Results and Discussion

5.3.1 Perception results

The perception measurement experiment was conducted to determine the effect of decreasing the stimuli size on the ability to differentiate between stimuli pair. The participant response data was analyzed by fitting the data to a logistic regression model using the GENMOD procedure in SAS (Statistical Analysis System) software. The data was assumed to follow a binomial distribution and the procedure assumed fixed block effects for each subject and then fixed effects for the stimuli size, texture pair used and their interaction. Bayesian analysis methods were used for fitting the logistic regression model and the mean probabilities of differentiating a given texture pair were obtained through an iterative procedure. The results of the perception measurement experiment can be seen in Figure 5.5.

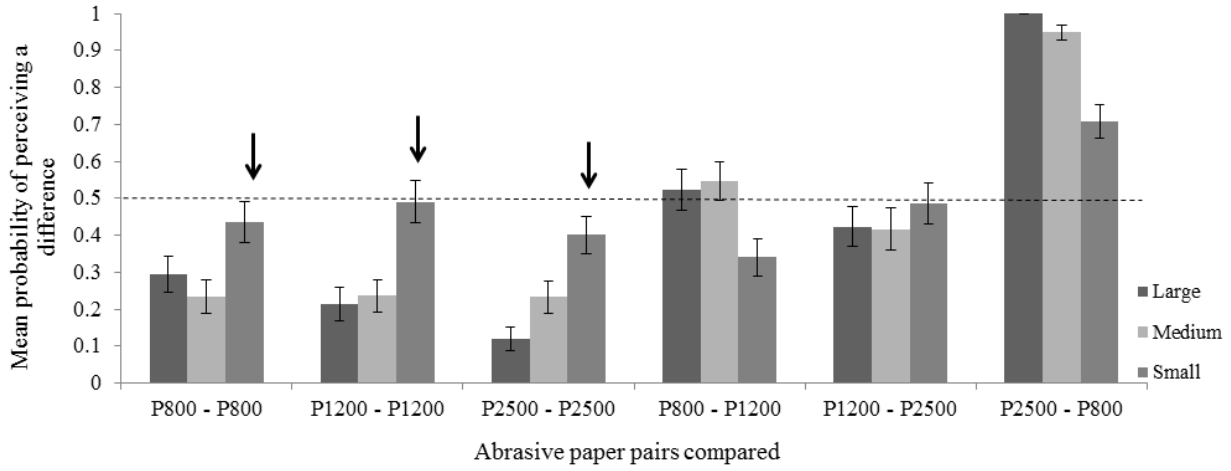

Figure 5.5 The effect of decreasing the size from large to medium on the mean probability of perceiving a difference (p) between two textures for all the 6 texture-pairings tested. Dashed line at p=0.5 indicates the probability of perceiving a difference by purely random choice.

The same possible theoretical mean probabilities for perceiving a difference discussed in Chapter 3 Section 3.3.1 are valid through the discussion here also. Briefly, the following three scenarios were possible.

1. Perceptually unbiased, where the participant perceives a difference between the texture samples purely by random choice and the mean probability $p = 0.5$.
2. Capability of perceiving a difference, where the participant correctly identifies different texture samples as different and the mean probability p in that case would be $0.5 < p \leq 1$. A given sample pair was reliably discriminated when the mean probability p was at least 0.7.
3. Capability of perceiving sameness, where the participant correctly identifies the same textures samples as same and the mean probability p in that case would be $0 \leq p < 0.5$. A given sample pair was reliably identified when the mean probability p was less than 0.3.

From the results of the perception measurement it can be seen that, of the three different-grit pair combinations tested, only P800 – P2500 pair was reliably discriminated at any size

(Large, medium or small). The reliable discrimination (mean probability of perceiving a difference was at least 0.7) was present for all three sizes tested, even though for the small size the mean probability value at 0.71 suggests that it was just at the threshold for reliable discrimination. Further, the mean probability of discrimination decreased with decrease in the sample size. For the P800-P1200 pair, the mean probabilities were similar to that of random choice at the large and medium sizes and at the small size, the participants were biased towards perceiving both the grits as identical. For the P1200-P2500 grit pair, the mean probabilities at all sizes were close to that of random choice. Based on these results, it is reasonable to state that the size change had the least effect on P1200-P2500 grit pair comparison and the most effect on P2500-P800 grit pair comparison.

All the same-grit pairs were reliably identified at the large and medium sizes (mean probability of perceiving a difference was at the maximum 0.3). The mean probabilities however, were closer to that of the random choice at the small size for all the three same-grit pairs. The effect of the decrease in the size from large to small was more evident for P2500-P2500 grit pair. Essentially, there was a decrease in the certainty /increase in the confusion with decrease in the size, especially from the medium to the small size for the same-grits pairs.

Overall, the mean probabilities of perceiving a difference for a given grit pair were similar for the large and medium samples and markedly different from those of the small samples except for the P1200-P2500 grit pair, indicating a general decrease in the ability to either reliably differentiate the different grit sample or reliably identify the same grit samples with decrease in the size of the texture samples. Based on these results, the following hypothesis is made: As a participant swipes a sample, his/her finger encounters the edge of the first texture

followed by its surface and then the edge of the second texture followed by its surface. For the larger samples, there was sufficient texture area for the surface parameters to influence the tactile judgments. However, as the texture area decreases the influence of the edge parameters on the perception decisions increases to a point where the decision was solely based on the edge parameters, which was suspected to have been the case with the small size samples. The nearly random choice probabilities for the same texture pair differentiation seen in Figure 5.5 suggest the same.

5.3.2 Human friction results

To investigate the potential roles of texture area and sliding friction on tactile discrimination, the friction and normal forces were measured for all the participants as they slid their index fingers in the similar conditions as the perception measurement. Figure 5.6 shows variation in friction and normal forces with sliding time in a single measurement for large, medium and small sample configurations of P2500-P800 grit pair for one of the participants. The results of previous work suggested that differences in the mean coefficients of finger friction between the grits could be indicative of the differentiability of surfaces through tactile perception[9]. From the human friction measurements, it was evident that there was a high variability among the participants in the applied normal loads and sliding speeds. Even for the measurements within a participant, it was observed that there was high variability in the applied normal load for different configurations, during different repetitions of the same configuration and sometimes even within the same measurement. This was in contrast with the observation by Smith et al. where participants adjusted normal forces to a constant value for optimal exploration of surface features[10]. Human fingerpad friction coefficient is complex variable known to be

influenced by multiple factors including the applied normal load[11-13] and sliding speed[14, 15]. Further, it is also important to take into consideration the effect of differences in mechanical properties of the skin among the participants on the finger friction[16]. Taking all of these factors into consideration, it became evident that using differences in the mean coefficients of friction for different textures from human friction data might lead to inaccurate conclusions. The trends in the friction and normal force curves from human friction data were examined instead.

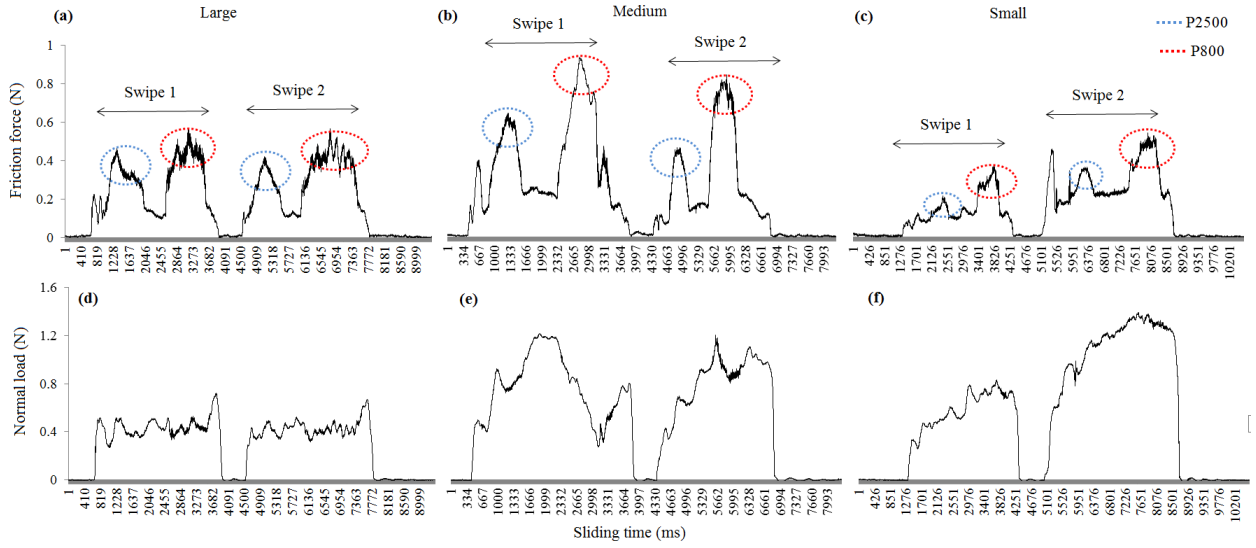

Figure 5.6 Variation of the friction force and the normal load with sliding time for P2500-P800 grit pair during a single measurement constituting two swipes for one of the participants. Friction force values for (a) Large, (b) Medium, and (c) Small sample configurations. Distinctive peaks in friction force corresponding to each of the textures were circled. Normal force values in the same measurement for (d) Large (e) Medium and (f) Small sample configurations can also be seen.

The friction force variation during a swipe was characterized by two distinctive peaks corresponding to the motion over the two textured samples, and by a flat valley-like region corresponding to the motion over the paper substrate outside of and between the textures. The friction force curves for the medium and small samples looked similar and were different from those of the large samples. For the large sample configurations, the peaks corresponding to the texture regions consisted of a sharp initial spike and followed by a decline in the friction settling

to a more or less constant value for rest of the texture's surface. For the medium and small configurations, the peaks in friction force curves constituted a sharp increase followed by a sharp decrease, with the peak being much sharper for the small sample configuration. Further, not all participants produced friction force data that was clean enough to identify distinct peaks in the small sample configuration. These trends in the data suggest that average friction for the large area texture samples may have been most influenced by the topography of the surface. For the small sample configurations, however, the quality and severity of the edge of the texture disks may have played a more dominant role. And, for the medium sample configuration both the surface topography and the edge height may have been responsible for the friction force trends. Because of the pronounced effect of the edges in the small samples, it is hypothesized that perception may be profoundly impacted by the edges with low texture area such that frictional cues are not able to be garnered to discriminate the textures. This behavior is borne out by the nearly random chance probability of correctly identifying small identical textures as such, shown in Figure 5.5

5.3.3 SEM images

Based on the human finger friction results and possible influence of the edge height and quality on the friction force trends, Scanning electron microscopy (SEM) imaging of the texture samples was performed to determine the edge height for each of the abrasive paper grits. Figure 5.7 shows the SEM images for each of the abrasive paper grits. The edge heights of the P800, P1200 and P2500 grits were 148 µm, 119 µm and 113.6 µm respectively. These measurements indicate that edge features are somewhat substantial, especially in relation to the small-diameter

samples. Therefore, one cannot easily dismiss the impact that edge-zone characteristics may have with respect to tactile discrimination of small features.

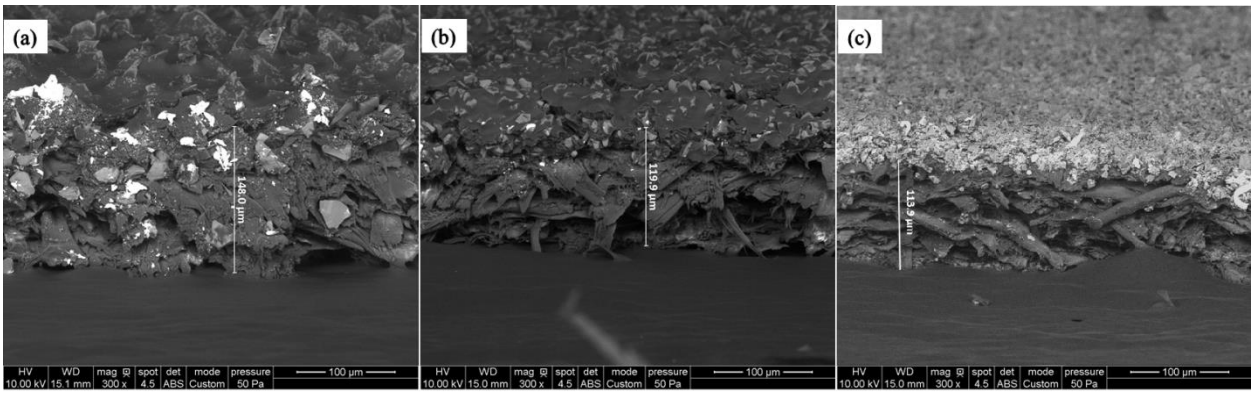

Figure 5.7 Scanning Electron Microscope images of the edges of the abrasive papers (a) P800, (b) P1200, and (c) P2500. All images were Back scattered electron images obtained at 300X and 85° tilt.

5.3.4 Silicone probe friction results

To avoid the subject to subject variation and obtain a more repeatable normal and friction force data, two silicone probes, a silicone sphere and a silicone finger replica were used to conduct friction tests with same texture sample sizes used in the perception and human friction experiments.

5.3.4.1 Silicone sphere

For the silicone sphere, the same sample configurations used in the human perception and friction measurements were used. For the silicone sphere, the shape of the friction force curves with respect to sliding times were similar to those observed in human friction measurements for all the three sizes. Initial normal force at the start of sliding was set at 1.5 N for all the measurements. As the sphere slid along the length of the sample surface, there was change in the surface height as the probe encountered the textured disks. This resulted in fluctuations in the normal load between 1.4 N and 2.7 N during each measurement period. Further there were also

slight variations in the normal load for different measurements possibly from small amount of bending of the probe in shear. However, plotting the friction force as a function of the normal load for different textures at each of the sample sizes tested (large, medium and small) showed an almost linear relationship between friction force and normal load (Figure 5.8). This indicates that a standard definition of coefficient of friction could be used as a reasonable means of normalizing data for comparison within the range of normal loads encountered here.

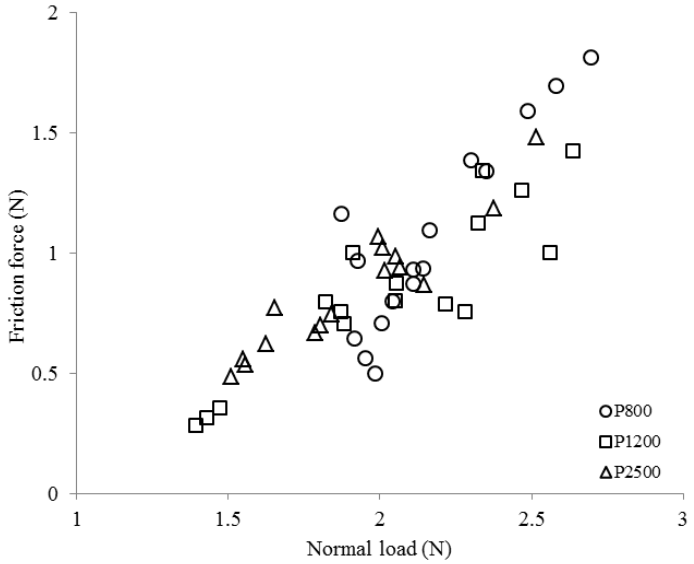

Figure 5.8 Variation of the friction force with the normal load for the small size samples of P800, P1200 and P2500 grit abrasive papers.

There were a total of 16 measurements for each of the different sized texture samples. For example, large-P800 texture had 16 measurements, during 8 of which P800 was the first surface the probe encountered and for the other 8 it was the second surface. It was observed that there was no variation in the coefficients of friction whether a particular texture was encountered first or second by the probe. All 16 measurements were pooled to obtain the mean and standard errors of the coefficient of friction for each size-texture combination of the samples. The results are shown in Figure 5.9. The mean coefficient of friction for the P800 grit was significantly different

from that of P1200 and P2500 grits at the large and medium sizes (p-values were less than 0.0005 all four cases), and but not at the small size (p-values were 0.13 and 0.54 respectively). The difference in the mean coefficients of friction between P1200 and P2500 grits was significant at the large size (p-value of 0.008) but not at the medium and the small sizes (p-values were 0.14 and 0.63 respectively). Comparing with the perception measurement data, these results bolster the hypothesis that the P800 is differentiated from the P2500 based on the difference in the friction experienced by the evaluator. However, this effect looks to become less pronounced as the grit sizes become closer and sample sizes get smaller. This suggests that significant differences in the coefficient friction alone might not indicate differentiability of two textures through perception, and that other factors such as the edge effects may become dominant in some cases. These results contrast previous work in some ways; however, the test conditions for perception were somewhat different between the two studies. One of the key differences being the samples were presented sequentially in the earlier study, and of very large area.

For all the three sample grits, the mean coefficients of friction at large and medium sizes were measured to be different from those at the small size. It is not likely that there are fundamentally different friction mechanisms between these sizes, and so it may be that the effect of the edge spikes again had a more profound effect on the measured frictional force for the small samples. This points out a limitation in the friction measurement techniques used in this study, but it also hints at what may be responsible for the small-texture-sample data in the perception study. No significant difference in the mean coefficients of friction was found between large and medium sizes for any of the textures. Comparing with the perception data for same-grit pairs, this decrease in the absolute value of the coefficient of friction with sample size combined with the insignificant differences in the coefficient of friction values between the grits

at small size, may have made it hard for the participants to decide which textures were identical and which ones were not, especially so for P1200 and P2500 grits, which were harder to differentiate between, even at larger sizes. This could possibly explain the decrease in certainty/ increase in the confusion in reliably identifying the same grit pairs.

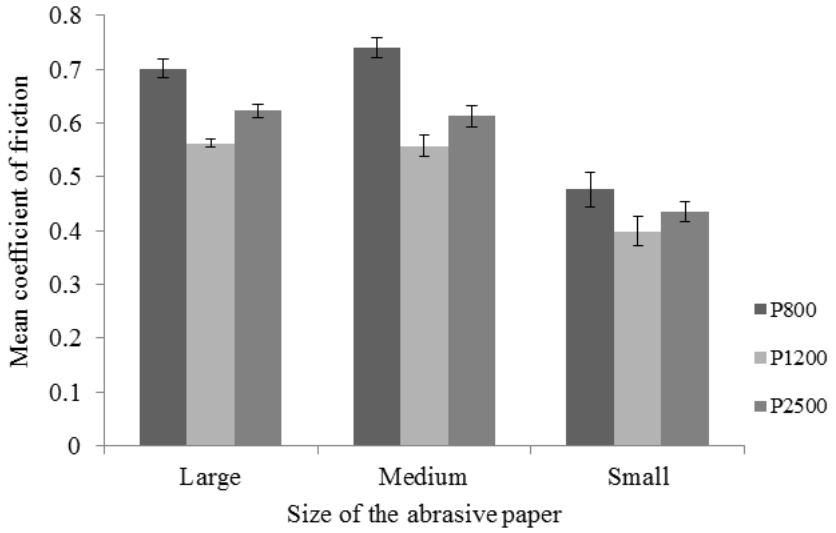

Figure 5.9 Variation of the mean coefficient of friction of the silicone sphere with the sample size for the P800, P1200 and P2500 grits.

5.3.4.2 Silicone finger replica

For the silicone finger replica, slightly different sample configurations from the ones used for the rest of measurements were used. Initial normal force was at the start of sliding was still set at 1.5N for all the measurements. However, as the finger replica slid along the length of the sample surface, there was a decrease in the normal load due to the bending of the finger opposite to the direction of the sliding. Results of the pre-tests showed that the decrease in the normal load due to bending stabilized at a distance of approximately 40mm from the starting point of sliding. The sample configurations were designed to accommodate for this bending effect. The decrease in the normal load due to bending was high as 0.8N. Further, there were also fluctuations in the

normal load during each measurement period due to changes in the surface height as the probe encountered the textured disks resulting in net normal load fluctuations in the range of 0.72 N – 2.2 N. There were a total of 8 measurements each for each size-texture combination and there was a non-linear variation of the friction force with the normal load in the normal load range encountered for the three textures at each of the sample sizes tested (large, medium and small). Figure 5.10 shows the results of silicone finger replica measurement as variation of the mean coefficient of friction with the size of the textures for different abrasive paper grits.

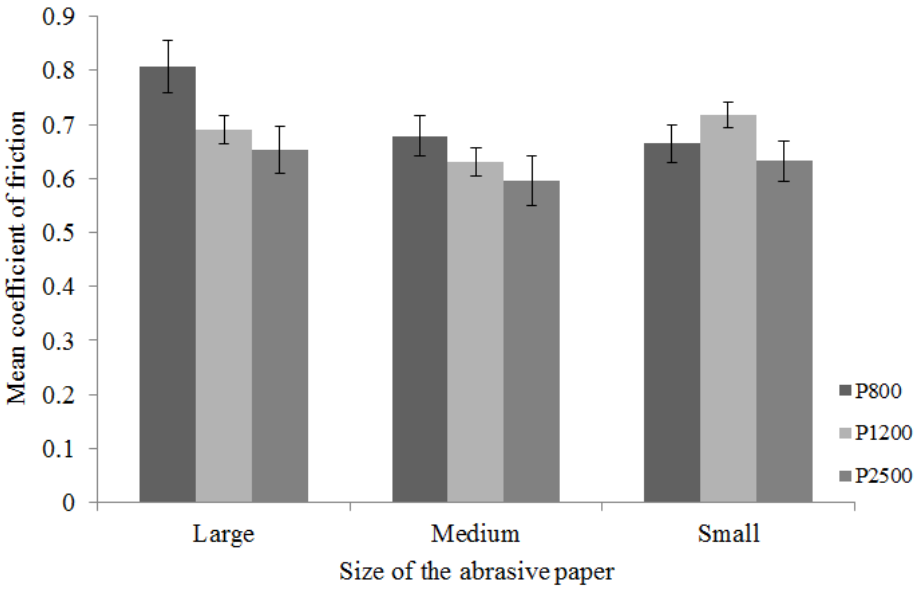

Figure 5.10 Variation of the mean coefficient of friction of the silicone finger replica with the sample size for the P800, P1200 and P2500 grits.

For the silicone finger the mean coefficient of friction for the P800 grit was significantly different from that P2500 grit at the large size (p-value of 0.02). Apart from that, there were no significant differences in the mean coefficients of friction between any of the textures at any of the sizes tested (p-values were greater than 0.3 for all other comparisons). Further, no change in mean coefficients of friction of the textures was observed as size the changed from large to medium to small for any of the textures. These results contrasts with the ones observed for the

silicone sphere. One possible explanation might be that the non-linearity in friction force associated with the normal load fluctuations was making mean coefficients of friction an unreliable measure to compare textures.

Further, due to the difference in the test configurations the normal force variation curves looked different from those from silicone sphere and the human friction measurements. This made it difficult to make any comparison with the perception and human friction measurements and draw meaningful conclusions.

5.4 Conclusions

This study investigated the effect of texture and sample area on tactile differentiability of three fine-grit abrasive papers and the role of friction in perception. The following conclusions can be made from the results of the study:

1. The mean probabilities of evaluators correctly perceiving a difference for a given pair of textures were similar for the large and medium sample sizes across grits. The discrimination results from the small samples indicated a significant decrease in the tactile differentiation ability of the participants with the decrease in the size of the samples. At the small sizes, evaluators did no better than random chance at determining if the pairs of textures where the same or different from each other.
2. The friction force curves from the human friction measurement indicated that the friction force values were influenced by the surface topography as well as the edge properties of the abrasive samples. The influence of the sample edge effects increased with the decreasing size of the texture samples, and suggests that the edge zone plays a greater

role than surface friction in the ability to perceive tactile differences between small texture areas.

3. Silicone sphere friction measurement data revealed that the coarsest grit, P800 had a significantly higher friction coefficient than the other two sample grits at large and medium sizes. This supports the hypothesis that friction plays a strong role in tactile discrimination at large and medium sample sizes. However, edge effects made friction measurements questionable for the smallest sample areas, and thus suggests that perceptive judgement may also be subject to errors in perceived friction due to edge effects.

5.5 Acknowledgements

The authors would like to acknowledge the Generational and Age Related Disabilities program within the Engineering Directorate of the National Science Foundation (Grant no. 1262797) for financial support of this investigation.

5.6 References

[1] Heller, M. Texture perception in sighted and blind observers. Perception & Psychophysics 45:49-54 (1989).

[2] LaMotte, R.H., Whitehouse, J. Tactile detection of a dot on a smooth surface: peripheral neural events. Journal of neurophysiology 56:1109 (1986).

[3] Johansson, R.S., Lamotte, R.H. Tactile detection thresholds for a single asperity on an otherwise smooth surface. Somatosensory & Motor Research 1:21-31 (1983).

[4] Lamb, G.D. Tactile discrimination of textured surfaces: psychophysical performance measurements in humans. The Journal of Physiology 338:551-565 (1983).

[5] Morley, J., Goodwin, A., Darian-Smith, I. Tactile discrimination of gratings. Exp Brain Res 49:291-299 (1983).

[6] Alary, F., Duquette, M., Goldstein, R., Elaine Chapman, C., Voss, P., La Buissonnière-Ariza, V., et al. Tactile acuity in the blind: a closer look reveals superiority over the sighted in some but not all cutaneous tasks. Neuropsychologia 47:2037-2043 (2009).

[7] Miyaoka, T., Mano, T., Ohka, M. Mechanisms of fine-surface-texture discrimination in human tactile sensation. The journal of the acoustical society of America 105:2485-2492 (1999).

[8] Skedung, L., Arvidsson, M., Chung, J.Y., Stafford, C.M., Berglund, B., Rutland, M.W. Feeling Small: Exploring the Tactile Perception Limits. Sci Rep 3 (2013).

[9] Chimata, G.P., Schwartz, C.J.: Tactile discrimination of randomly textured surfaces: effect of friction and surface paramateres. Place (2016)

[10] Smith, A., Gosselin, G., Houde, B. Deployment of fingertip forces in tactile exploration. Exp Brain Res 147:209-218 (2002).

[11] Derler, S., Gerhardt, L.C., Lenz, A., Bertaux, E., Hadad, M. Friction of human skin against smooth and rough glass as a function of the contact pressure. Tribology International 42:1565-1574 (2009).

[12] Childs, T., Henson, B. Human tactile perception of screen-printed surfaces: Self-report and contact mechanics experiments. IMechE Proceedings 221:427-441 (2007).

[13] Tomlinson, S.E., Lewis, R., Carré, M.J. The effect of normal force and roughness on friction in human finger contact. Wear 267:1311-1318 (2009).

[14] Pasumarty, S., Johnson, S., Watson, S., Adams, M. Friction of the Human Finger Pad: Influence of Moisture, Occlusion and Velocity. Tribol Lett 44:117-137 (2011).

[15] Dinç, O.S., Ettles, C.M., Calabrese, S.J., Scarton, H.A. Some Parameters Affecting Tactile Friction. J Tribol 113:512 (1991).

[16] Liu, X. Understanding the effect of skin mechanical properties on the friction of human finger-pads. (2013).

CHAPTER 6. GENERAL CONCLUSIONS

Based on the research objectives set out at the beginning of this dissertation, the conclusions from the current research work could be divided into two categories: 1) Pertaining to the psychophysical aspects of discriminative touch, and 2) Pertaining to the development of synthetic skin simulant.

Studies described in Chapters 3 and 5 focused on the psychophysical aspects. In Chapter 3, tactile differentiability of six fine-grit abrasive papers was measured as mean probability of perceiving a difference between different grit-pairs. The mean probability values indicated that the six textures investigated fall into three clearly differentiable categories. Surface parameter and finger friction measurements were also obtained for the same six textures. Examining the perception results together with surface property measurements revealed that, in order to clearly perceive a difference between two fine textured surfaces, there should be significant difference in the measures of distribution of distinct topological features like mean spacing of the profile peaks and the coefficients of friction of the textured surfaces compared. Further, differences in the average roughness measures (like root mean square roughness) were found to be not representative of the ability of individuals to discriminate between fine textured surfaces. In Chapter 5, three of the textures which were clearly differentiated in the previous study were selected and the effect of the size of the texture samples on their tactile discriminability was investigated. Friction measurements for participants' fingers and silicone probes against the abrasive papers were also obtained. The results indicated a significant decrease in the tactile differentiation ability with the decrease in texture size. The friction force curves from the human and silicone sphere friction measurements indicated that the friction force values were influenced

by the surface topography as well as the edge properties of the textures. The influence of the edge properties increased with the decreasing texture size on friction, and consequently on perception, leading to erroneous tactile judgements at small sizes.

Chapters 2 and 4 focused on development of synthetic skin simulant and identifying factors essential to design of the simulant. In Chapter 2, a two-layer elastomeric skin simulant was developed and the relationship between applied normal load and number of cycles of reciprocating motion required for blistering in the simulant was studied. The blistering behavior of the simulant was similar to that of human skin. A fracture mechanics based crack growth model showed some agreement with the friction-induced blistering. It was also evident from this study that a comprehensive knowledge of factors affecting skin friction is reuired to develop a simulant that can accurately estimate skin damage. In chapter 3, coefficient of friction of four probing surfaces, human index finger pad, silicone replicas of the finger with and without fingerprints, and a smooth silicone sphere were compared to identify the roles of shape of the finger, elastic properties and fingerprints on fingerpad friction. The results of the study indicated that the fingertip coefficient of friction when interacting with textured surfaces of small rigid elements (<50 μm) could be a summation of adhesion, deformation and the interlocking components. The shape of the finger was responsible for increase in contacting surface area, which further affected the adhesion and deformation components of friction. The presence of fingerprint ridges possibly added an interlocking contribution to the overall coefficient of friction. The contribution of interlocking friction can vary with multiple factors like the shape and size of the contacting asperities, sliding direction of the finger and the angle of sliding. And, changing the elastic properties could impact all the three components of friction.